Development and Analysis of Various CO_2 Capture and Utilization Pathways for DME Production

Angelica Maria Cabarcas Toro

A Thesis

In the Department of

Chemical and Materials Engineering

Presented in Partial Fulfillment of the Requirements

For the Degree of

Master of Applied Science (Chemical Engineering)

at

Concordia University

Montréal, Québec, Canada

April 2024

CONCORDIA UNIVERSITY

School of Graduate Studies

This is to certify that the thesis prepared

By: Angelica Maria Cabarcas Toro

Entitled: Development and Analysis of Various CO_2 Capture and Utilization Pathways for DME Production

and submitted in partial fulfillment of the requirements for the degree of

Master of Applied Science (Chemical Engineering)

Complies with the regulations of the University and meets the accepted standards with respect to originality and quality.

Signed by the final Examining Committee:

_____ Chair

Dr. Alex De Visscher

_____ Examiner

Dr. Ivan Kantor

_____ Supervisor

Dr. Yaser Khojasteh-Salkuyeh

Approved by _____

Dr. Sana Jahanshahi Anbuhi, Graduate Program Director

April 2024 _____

Dr. Mourad Debbabi, Dean Gina Cody School of Engineering and Computer Science

ABSTRACT

Development and Analysis of Various CO_2 Capture and Utilization Pathways for DME Production

Angelica Maria Cabarcas Toro

Sustainable energy resources are required to address the rising demand for energy while promoting economic stability. Dimethyl ether (DME) is a second-generation environmentally friendly fuel that offers an alternative for replacing traditional petroleum fuels. In this project, we designed three distinctive pathways for the synthesis of DME from syngas. A comprehensive analysis was also conducted, including the production and thermal efficiency, economic, and environmental impact perspectives, to evaluate the outcomes of each pathway. For each section, a rigorous process simulation was conducted using Aspen Plus and considering detailed catalytic reaction modelling.

According to our results, the production rate of the Direct Method, yielding 1.21 kg DME/kg CO_2, demonstrated an improvement to 1.37 kg DME/kg CO_2 with the integration of the Reverse Water Gas Shift (RWGS) process. Notably, the Indirect Model emerged as the most favorable, exhibiting a superior outcome with a DME yield of 1.95 kg DME/kg CO_2.

Conducting a Techno-Economic Analysis (TEA) unveiled that the Indirect Method stands as the most economically advantageous, attributed to its lowest Minimum Selling Price (MSP) of 2465 $/tonne and the highest annual revenue of 437 $Million.

Upon assessing the environmental impacts of the pathways through the TRACI 2.1 methodology, it was revealed that the Indirect Method requires the lowest amount of Greenhouse Gas (GHG) avoided credits, valued at 0.164 $/kg$CO_2$, due to the proximity of the MSP and the Market Price (MP).

The combination of superior yield and economic viability outcomes, positions the Indirect Method as the most competitively advantageous approach in this research.

Acknowledgments

I want to express my deepest gratitude to Dr. Yaser Khojasteh, who has given me his unconditional support and guidance. His direction uplifted my knowledge and encouraged my spirit to endure all challenges. Your commitment and dedication to academia are admirable; you have forever made a positive impact on my life.

I will forever be thankful to Khadijeh Barati, for the strength and faith you bestowed upon me. Your unwavering support gave me the certainty that I could achieve my goals.

I would like to express my deepest gratitude to Imelda Padilla. Without her relentless guidance, love, and protection, the completion of this dissertation would not have been possible. Thank you for being my pillar since the beginning of this journey.

I am also grateful to Jeison Moscote, Kevin Paquette, and my CSTAR friends for your valuable advice, contributions, and assistance.

Lastly, I'm extremely grateful to my family for giving me the courage to continue and reminding me that all sacrifices come with great rewards.

Table of Contents

List of Figures vii
List of Tables viii
Nomenclature ix
1. Introduction 1
1.1. Background and Motivation 1
1.2. Research Objectives 2
1.3. Thesis Layout 3
2. Literature Review 4
2.1. Carbon Capture Storage and Utilization 4
2.2. DME Production 6
2.2.1. Synthesis Methods 6
2.2.1.1. Direct Synthesis 6
2.2.1.2. Indirect Synthesis 6
2.2.2. Types of Reactors 7
2.2.2.1. Fixed-bed Reactors 7
2.2.2.2. Slurry Phase 7
2.3. Reverse Water Gas Shift 8
2.4. Summary 10
3. Process Description 11
3.1. CO_2 Capture Unit 13
3.2. CO_2 Compression Unit 15
3.3. Direct Method 16
3.3.1. Baseline (Direct Method) 16
3.3.1.1. Reactor Design 19
3.3.1.2. Product Recovery 21
3.3.1.3. Distillation Columns 22
3.3.1.4. Heat Demand 22
3.3.1.5. Refrigeration Duty 23
3.3.2. Modified (Direct Method with RWGS) 23
3.3.2.1. Reactor Design 26

3.4. Indirect 27
3.4.1. MeOH Production Unit 27
3.4.1.1. Heat Demand 31
3.4.2. DME Production Unit 31
3.4.2.1. Reactor Design 34
3.4.2.2. Distillation Columns 34
4. Results and Evaluation 35
4.1. Production Results 35
4.2. CO_2 Utilization 36
4.3. Hydrogen Consumption 37
4.4. Process Energy Demand 38
4.5. Overall Efficiency 40
5. Techno-Economic Analysis 41
5.1. Assumptions 41
5.2. Capital Investment Costs 42
5.3. Operating Costs 44
5.4. Economic Evaluation 45
5.5. Sensitivity Analysis 46
6. GHG Analysis 49
7. Conclusion 54
7.1. Future Works 55
8. Appendix 56
8.1. Capital Expenditures 56
8.2. Operational Expenditures 57
8.3. Net Present Value 58
9. Bibliography 59

List of Figures

Figure 1. Simplified block diagram of the (a) Conventional ammonia production process, (b) Ammonia process integrated with the CO_2 utilization unit 11
Figure 2. Simplified block diagram of the integrated CO_2 capture and utilization based on (a) Direct DME production, (b) Direct DME production with RWGS, and (c) Indirect DME production via methanol production 12
Figure 3. Schematic of the CO_2 Capture Unit using MEA solvent 13
Figure 4. Schematic of the CO_2 Capture Unit with hydrogen injection and heat pump 14
Figure 5. Schematic of the CO_2 Compression Unit 15
Figure 6. Process Flow Diagram of Direct Baseline Model 16
Figure 7. Impact of the DME reactor temperature and DME produced/inlet CO_2 ratio 20
Figure 8. Sensitivity analysis of DME reactor for number of tubes vs DME produced/CO_2 in the feed and pressure drop 20
Figure 9. Process Flow Diagram of Direct Modified Model with RWGS 23
Figure 10. Conversion of CO_2 in $CuO/ZnO/Al_2O_3$ catalyst reactor and equilibrium vs temperature 25
Figure 11. Process Flow Diagram of Indirect Model; MeOH Unit 27
Figure 12. Process Flow Diagram of Indirect Model; DME Unit 31
Figure 13. Sensitivity analysis of DME reactor for inlet feed temperature versus DME out/MeOH in 33
Figure 14. Production rate of pathways 36
Figure 15. Carbon dioxide utilization of pathways 37
Figure 16. Hydrogen consumption of pathways 38
Figure 17. Overall energy demand of pathways 39
Figure 18. Efficiencies across pathways 40
Figure 19. Effect of electricity price of provinces on Minimum Selling Price of DME 47
Figure 20. Effect of Electricity Rate on the Minimum Selling Price of DME 48
Figure 21. Scope of the LCA of the pathways 49
Figure 22. GHG impact contribution by province, (a) without avoided emissions of MeOH, and (b) with avoided emissions of MeOH 51
Figure 23. Avoided GHG credit required of pathways required for different carbon intensity ... 52

List of Tables

Table 1. Raw syngas to the Amine unit 13
Table 2. Process data and simulation results of the Amine unit 15
Table 3. Coefficients of equilibrium constants of reactions equations (6), (8), (9) and (10) [39,46] 18
Table 4. Kinetic parameters of CuO-ZnO-ZrO_2@SAPO-11 core-shell catalyst for DME production [45,46] 18
Table 5. Operating conditions of DME Reactor and Catalyst [45] 19
Table 6. Operation conditions for distillation columns of direct model 22
Table 7. Operating conditions of RWGS Reactor and Catalyst [33] 24
Table 8. Kinetic parameters of CuO/ZnO/Al_2O_3 catalyst for CO production [33] 26
Table 9. Operating conditions of MeOH Reactor and Catalyst 28
Table 10. Equilibrium constant and activation energy for ETOH and DME production rate [55] 29
Table 11. Kinetic values for MeOH and RWGS production rate [55] 29
Table 12. Operation conditions for distillation columns of MeOH unit in the indirect model 30
Table 13. Operating conditions of DME Reactor and Catalyst Indirect [57] 32
Table 14. Operation conditions for distillation columns of DME unit in the indirect model 34
Table 15. Overall mass balance and energy demand of pathways 35
Table 16. Economic evaluation assumptions 42
Table 17. Capital investment parameters used for CAPEX estimation [59] 43
Table 18. Operating cost parameters used for OPEX estimation [59] 45
Table 19. Economic analysis summary of three pathways 46
Table 20. Reference processes from Ecoinvent database 50

Nomenclature

CCS	Carbon capture and storage
CCU	Carbon capture and utilization
DME	Dimethyl ether
MeOH	Methanol
LPG	Liquified petroleum gas
GHG	Greenhouse gas
MEA	Mono-ethanol amine
PEM	Proton exchange membrane
HHV	Higher heating value
BFW	Boiler feed water
LCA	Life cycle assessment
TRACI	Tool for reduction and assessment of chemicals and other environmental impacts
CEPCI	Chemical engineering plant cost index
MSP	Minimum selling price
TWSE	Total operating and maintenance wages, supervision, and engineering expenses
CAPEX	Capital expenditures
OPEX	Operating expenditures

1. Introduction

In an era marked by an increasing demand for sustainable energy alternatives, the development of innovative solutions has become a vital concern. Due to the environmental challenges and the critical nature of reducing greenhouse gas (GHG) emissions, our research aims to develop effective pathways for the synthesis of dimethyl ether (DME) from the application of carbon chain utilization (CCU). This research emerges not only as a response to the demand for more environmentally friendly fuels but also to redefine the conventional frameworks of DME production.

1.1. Background and Motivation

Dimethyl ether (DME) is an organic compound represented by the formula CH_3OCH_3. While it is a highly flammable gas under standard atmospheric conditions, it transforms into a liquid phase when subjected to 5 bar or more. Therefore, DME is usually stored in its liquid state [1].

DME is a great option for diesel engines, as it has a very high cetane number and lacks carbon-to-carbon bonds. This makes it easy to ignite and results in efficient combustion with almost no particulate matter emissions. It has similar vapor pressure to LPG, which also makes it a good fuel option. Furthermore, DME is compatible with the existing infrastructure for transportation and storage of LPG, making it a valuable alternative energy [1,2]. It is noteworthy that dimethyl ether does not exhibit any carcinogenic, teratogenic, mutagenic, or toxic properties [3].

The primary practical uses of this versatile fuel are to replace propane in residential cooking systems that utilize LPG, and to operate as a fuel source in gas turbine power generators. In addition, DME exhibits potential as a substitute fuel for transportation, being compatible with both gasoline and diesel engines [1].

Despite its promising advantages and potential to penetrate the gas and liquid fuel market, one of the driving factors for DME application is that DME can be produced from a wide range feedstock, such as fossil fuels (natural gas, crude oil, and coal) [1]. Several works have been done to study the production of DME from different biomass and biogas feedstock from a life-cycle impact perspective, comparing it to natural gas produced DME, but those studies have inconsistent considerations, units and scope, so Lee et al. [4] investigated the emissions of five DME production pathways, using fossil and renewable sources, comparing them to gasoline and diesel fuels. Their

research findings suggest that the production DME from natural gas results in elevated greenhouse gas (GHG) emissions when compared to conventional fuels like gasoline and diesel. Specifically, in the context of diesel, the disparity in GHG emissions is notable, with a relative increase of around 5%. However, alternative pathways for DME production utilizing resources such as landfill gas (LFG), manure waste streams (MANR), and black liquor (BL) demonstrate substantial GHG emission reductions, ranging from 46% to 99%. Despite these promising reductions, it is essential to note that such pathways are typically associated with small-scale DME plants. While these alternative pathways contribute to mitigating GHG emissions, although to a lesser extent, they nonetheless remain sources of emissions.

The other alternative route is based on DME production using CO_2 capture and utilization (CCU), which assists us mitigate the problem of carbon dioxide emissions while taking advantage of them [5]. In recent years, CCU processes have been promoted, specifically to convert CO_2 to fuel or chemicals by renewable energy-derived H_2 [6]. Therefore, our research addresses this need by exploring the synthesis of DME from syngas, addressing the gaps in current DME production methods. Our goal is to present a viable, sustainable, and economically sound alternative.

In this project, we designed and analyzed three pathways - the Direct Method, Direct Method with Reverse Water Gas Shift (RWGS), and Indirect - each presenting promising opportunities and challenges. Our goal is to effectively investigate this unexplored domain while prioritizing economic sustainability, environmental friendliness, and energy efficiency.

1.2. Research Objectives

Our research objectives are multifold. Primarily, we aim to develop an efficient CCU-DME pathway by designing, simulating, and performing a comparative analysis of the Direct Method, Direct Method with RWGS, and Indirect Method pathways. This assessment encompasses factors such as environmental impact, energy efficiency, and economic feasibility, in addition to production rates. The research progresses in several stages: hypothesis formulation, pathway design and simulation using Aspen Plus® version 12.1, data collection based on a standardized initial feed, and analysis. This analysis spans production rates, carbon dioxide utilization, hydrogen consumption, energy demand, energy efficiency, techno-economic factors, and a greenhouse gas analysis utilizing the OpenLCA software version 1.11.

1.3. Thesis Layout

Following this introduction, subsequent chapters will delve into the detailed analysis of the Direct Method, Direct Method with RWGS, and Indirect pathways. In Chapter 2, an overview of the current state of CCU processes and the production of DME is presented. Chapter 3 explains in detail the process description involved in the three pathways of DME production. In Chapter 4 the outcomes are assessed, such as production results, carbon dioxide utilization, hydrogen consumption, process energy demand, and overall efficiency. Chapter 5 provides a techno-economic analysis of these pathways. Chapter 6 provides the scope to include environmental impacts resulting from the pathways, considering different geographical locations and distinct sources of electricity. Lastly, Chapter 7 summarizes the key results of this research and its conclusions.

2. Literature Review

2.1. Carbon Capture Storage and Utilization

Carbon capture and storage (CCS) is the process where CO_2 is separated by a capture technology such as physical, chemical or membrane separation and stored underground [7]. It was first implemented at a large scale with the Sleipner and Snøhvit gas fields projects in Norway. These facilities were designed to remove CO_2 from the liquified natural gas, then compress and inject it below the seafloor to permanently dispose. There have been questions about whether this technology is sufficient to secure greenhouse gases on a scale, particularly since there have been incidents observed, such as having the deposited CO_2 moved rapidly and unexpectedly to unidentified areas, or the concerns about the storage capacity for long-term operation [8]. Moreover, there are concerns about the profitability of CCS pathways, particularly since it's an unprofitable activity that requires large capital investment [9,10].

The technique of converting CO_2 into other compounds through chemical interactions with hydrogen is known as carbon capture and utilization (CCU). This is one of the most efficient carbon-neutral (or even carbon-negative, depending on the product) solutions for the decarbonization of heavy industries [7]. CCU is one of the solutions to mitigate greenhouse gas emissions and was recognized by the United Nations in the Paris Agreement in 2015 [11]. The Paris Agreement sets the goal to limit global warming to well below 2 ˚C compared to pre-industrial levels by reducing emissions to 40 gigatonnes by 2030.

Reducing the energy consumption of CCU pathways is one of the key challenges to be addressed prior to the commercialization of such technologies. Different technologies of carbon capture, such as post-combustion, pre-combustion and oxy-fuel combustion, are described and summarized by Cuéllar-Franca et al. [10] which can be used in both CCS or CCU processes. Pre-combustion capture refers to capturing the CO_2 that is generated as an unwanted byproduct in an intermediate reaction of a process [10,12]. Ammonia generation is one instance [10,13]. In the synthesis of ammonia, CO_2 and H_2 are co-produced during steam reforming and must be separated to prevent interfering with the production process, the conventional absorption is typically through mono-ethanol amine (MEA), despite having a high energy consumption [10,14]. This problem has been addressed by different researchers using various technologies. Machida et al. [6] investigated the impact of injecting H_2 to the bottom of the desorber as a stripping gas for solvent regeneration,

reducing the regeneration temperature, and achieving energy savings by improving heat recovery. Khojasteh et al. [15], explored changing operating parameters, concluding that increasing the pressure of the absorber, increasing the concentration and decreasing the temperature of the solvent, results in a lower energy requirement.

The second challenge is defining a suitable CO_2 conversion end product to be competitive with conventional processes, with minimum financial support. Different routes of the CCU process are currently under development, such as the CCU-MeOH production, the first large-scale plant is located in Iceland [16], with a capacity of 4000 tonne/year. The facility captures the flue gas from a near by geothermal power plant, transforms it into syngas, and then it's transformed into MeOH, this flue gas is naturally present in geothermal fluids, and is formed mostly of CO_2, H_2S, CH_4. Yang et al. [17] performed an analysis of a CO_2-MeOH plant using MEA as solvent, while integrating heat and mass, their research suggests that by applying such integrations, there is a reduction in environmental impacts and operational expenditures compared to conventional MeOH production processes, and that the economic viability depends strongly on the cost of electricity. Likewise, the production of synthetic natural gas (SNG) from CO_2 offers another route for CCU, Chauvy et al. [18] studied the viability and environmental impacts of implementing carbon capture at a cement plant and using its flue gas in the production of synthetic natural gas (SNG). They concluded that by implementing this route, there is a reduction of the net CO_2 emissions by 66%, while producing 400 kg/h of SNG using the data generated from the simulation of the process in Aspen Plus software. While there are several works focused on the CCU-MeOH and SNG, there is limited research on alternative chemicals and fuels. One of the key challenges is the production cost of the product. For instance, according to the TEA results of the CCU-MeOH pathway [19], the production cost of methanol can be 2 to 3 times its market price. One of the alternative CCU routes is the conversion of CO_2 to DME. Besides the benefits and advantages of DME as the CCU product, the development of efficient CCU-DME pathways can enhance the potential market for the use of CO_2 and its global demand. There are two different routes for the synthesis of DME: direct and indirect methods.

2.2. DME Production

2.2.1. Synthesis Methods

2.2.1.1. Direct Synthesis

In the direct synthesis method, DME is synthesized directly from syngas containing H_2, CO, and CO_2 through specific reactions, such as methanol synthesis, methanol dehydration and water gas shift. This method allows for higher CO conversion and simpler reactor design, resulting in lower production costs for DME [20,21]. However, the separation process for high-purity DME can be more complex due to the presence of unreacted syngas and produced CO_2. Additionally, the water-gas shift reaction in this method consumes CO, making it less suitable for commercial purposes [20]. This challenge is observed in an experimental study performed by Shukurov et al. [22], where H_2O and CO_2 accumulated and were considered disadvantageous for the process. Hence, it is critical to have proper operating conditions to enhance the DME production rate. Vakili et al. [23] tried to modify the operating conditions using a differential evolution (DE) optimization algorithm for an industrial-scale fixed bed reactor and achieved 4.84% more of DME productivity.

Carrero et al. [5] conducted a simulation-based optimization using Aspen HYSYS to produce DME from dry reforming of natural gas. They analyzed different process flow pathways to identify the most cost-efficient way to maximize the profitability of the DME plant. Additionally, they conducted a life cycle assessment (LCA) using the ReCiPe EndPoint method. According to their results, the process in its optimal configuration can have a potential profit of 59 $Million/year, while emitting 0.5 $kgCO_2eq/kgDME$. Moreover, Poto et al. [24] performed an analysis of DME production using the Aspen Plus and Matlab tools. Their study focused on evaluating the operational and economic impacts of using a membrane reactor (MR) in contrast to the conventional methods. In their scope, neither the CO_2 capture and compression units, nor the H_2 generation unit were considered. Their results showed an increase in a single pass conversion of 16%, a negligible reduction in the capital expenditure (CAPEX), and a 18% reduction in the operational expenditure (OPEX).

2.2.1.2. Indirect Synthesis

The indirect synthesis method involves a two-step process. Initially, methanol is generated from syngas in a catalytic fixed-bed reactor, followed by purification stage using two distillation

columns. Subsequently, in a separate reactor, this purified methanol is converted into dimethyl ether. This method has been used in industrial settings and is well-established for DME production. The big issue with this process is the substantial upfront costs for different units like reactors, columns, and heat exchangers. They require a lot of space in a plant and have a high energy demand to run [20,25]. In an attempt to optimize the production of DME using this method, Farsi et al. [26] simulated it using genetic algorithm (GA) programming, increasing the MeOH conversion 4.70% Most of the articles reviewed by Azizi et al. [20] are conducted on temperatures ranging from 200 to 300 °C and pressures up to 70 bar. These studies commonly use fixed-bed reactors due to their ease of operation. In summary, the direct synthesis method offers cost and reactor design advantages but struggles to achieve high purity DME. On the other hand, the indirect synthesis method, while established and widely used, may be less energy-efficient. Further research and development are necessary to improve the efficiency, selectivity, and sustainability of both methods in DME production.

2.2.2. Types of Reactors

2.2.2.1. Fixed-bed Reactors

Fixed-bed reactors are commonly used in laboratory or pilot-scale operations due to their simple design and cost-effectiveness [20,27]. These reactors consist of a stationary catalyst bed through which reactants pass. However, a drawback of fixed-bed reactors is the challenge of controlling temperature, especially in adiabatic fixed-bed reactors, which can impact the overall reaction rate.

2.2.2.2. Slurry Phase

Slurry phase reactors are another type commonly used in commercial direct DME synthesis technology. In these reactors, syngas is dispersed as the bubble phase in a solvent that suspends the catalyst. Slurry phase reactors offer advantages such as lower investment costs, better heat transfer, and the potential for large-scale DME production. However, there are challenges associated with slurry phase reactors, such as limitations in mass transfer between phases, the complexity of equipment required (including a recycling system and gas-liquid separator), and the loss of catalyst particles from the reactor [20].

We can agree with Azizi et al. [20], that despite the amount of studies on DME production available in the literature, there is still a gap regarding the economic analysis, life cycle assessment and efficiency of the complete process, with the potential benefit of the RWGS process being overlooked. Peinado et al. [28] evaluated the differences in the production of DME from the direct and indirect methods, but only compared thermodynamics, kinetics, reactor types, heat and mass transfer, without comparing the economic and LCA aspects. Likewise, Nakyai et al. [29] compared the direct and indirect synthesis methods for DME production, applying an exergoeconomic and environmental analysis from the syngas produced of biomass, concluding that the ideal case would only have CO, since the presence of CO_2 in the feed affected the DME yield, obtaining an energetic efficiency of 35.79%. Similarly, Wu et al. [30] looked at five different scenarios, comparing two direct, two indirect methods, and one mixed method. They studied how having three reactors in series, using heat integration, recycling methanol, and getting H_2 from different sources affected the CO_2 conversion and economic viability. They found that the indirect method with heat integration was best at reducing CO_2 emissions, cutting them by -1.7 $kgCO_2eq/kgDME$. However, even with different H_2 sources, the process still isn't economically attractive because of the high prices of H_2.

2.3. Reverse Water Gas Shift

Despite several works for enhancing the yield and conversion of CCU pathways, the low conversion rate of CO_2 is still a challenge, particularly as CO_2 is an extremely stable molecule with a high dissociation energy (750 kJ mol^{-1}) [31]. The conversion of CO_2 into CO is one alternative approach to improve the conversion of CO_2. This conversion is achieved using the catalytic endothermic reverse water gas shift (RWGS) reaction, which consists of the conversion of carbon dioxide and hydrogen into carbon monoxide and water. The CO_2 conversion can be improved by increasing the temperature and H_2/CO_2 ratio [31], which makes the RWGS an energy-intensive reaction. This process usually takes place in a packed-bed reactor with metal/alumina catalysts [32,33].

In 1914, Carl Bosch and Wilhelm Wild first detected the RWGS reaction while attempting to create hydrogen gas from steam and carbon monoxide on an iron oxide catalyst [34]. Numerous efforts have been made to optimize the RWGS process. Dzuryk et al. [33] achieved 98.1%

conversion by incorporating a water-permeable membrane into the reactor to facilitate water removal, employing a counter-current configuration with H_2 permeation. Zhuang et al. [32], on the other hand, obtained a 46% conversion by employing a Ru-promoted Cu/ZnO catalyst, although the corresponding equilibrium conversion at the same temperature was 55%. In contrast, the baseline Cu/ZnO catalyst only yielded a 17% conversion under identical conditions. Similarly, Shekari et al. [35] addressed the limitations of commercial catalyst reactors in achieving maximum yields, considering factors such as thermodynamic equilibrium and maintenance costs. They achieved a 75% CO_2 conversion in a single pass in their experimental setup, using a reactor without catalysts. Their approach involved employing a hydrogen oxyflame feed, facilitated by an oxygen-carbon dioxide mixture as an oxidizer.

Moreover, the RWGS reaction serves as a pivotal intermediate stage in numerous CO_2 hydrogenation processes, particularly in the production of light olefins such as ethylene. For instance, when utilizing iron (Fe) catalysts, the process exhibits notable variations based on temperature. At temperatures below 320 °C, the catalyst tends to yield carboxylic acids. However, surpassing the 320 °C threshold leads to a significant shift in product formation, favoring the production of light olefins, as it was mentioned by Hu et al. [36].

In addition, carbon dioxide hydrogenation to form methanol via RWGS (CAMERE) is also utilized. Park et al. [37] demonstrated the effectiveness of this method by achieving a 43% conversion of CO_2 into methanol at a temperature of 600°C, employing a ZnO/Al_2O_3 catalyst.

Besides the applications previously mentioned, Ateka et al. [38] proposes CO_2 hydrogenation routes, such as RWGS, to enhance the production of DME, taking into consideration that CO is more reactive than CO_2, but the reaction is carried out under unfavorable conditions due to higher content of CO_2 in the syngas. In another study [39], Ateka et al. found that decreasing the concentration of CO_2 in the feed results in an advantage for DME conversion. The scope of their research is focused on temperatures from 200 to 400 °C, with an H_2/CO_X ratio of 3, at pressures from 10 to 40 bar, with different CO_2/CO_X ratios. They obtained the highest conversion in the absence of CO_2, at 40 bar and 200 °C.

2.4. Summary

Overall, many studies have looked into different ways to make DME production more energy efficient, cheaper, and to have a lower impact in the environment. However, the low conversion and production costs remain the key challenges. Particularly as only a few works focused on the process design and analysis of the use of CO_2 as the feedstock of the DME production processes. In this work, we tried to improve the performance of the CO_2 utilization process for DME production by focusing on different aspects. First, the CO_2 capture section is improved by incorporating hydrogen as the stripping agent and using a heat pump to reduce the overall energy demand. Second, two different pathways are modelled and analyzed from GHG emissions and production cost viewpoints: Direct and Indirect methods. Finally, the effects of implementing RWGS process in the Direct Method are investigated by performing a detailed process simulation and techno-economic analysis covering all units of production.

3. Process Description

This thesis focuses on developing an integrated process for utilizing CO_2. The simplified schematic of the conventional and modified Ammonia plants is shown in Figure 1. In the proposed process, the current CO_2 removal unit is modified by injecting hydrogen into the amine unit, which then transfers the captured CO_2 to the CO_2 utilization unit. By using this method, we aim to reduce the energy demand of the CO_2 capture section. Hence, in this chapter, the CO_2 capture unit is first described, and then, we will discuss the DME production pathways.

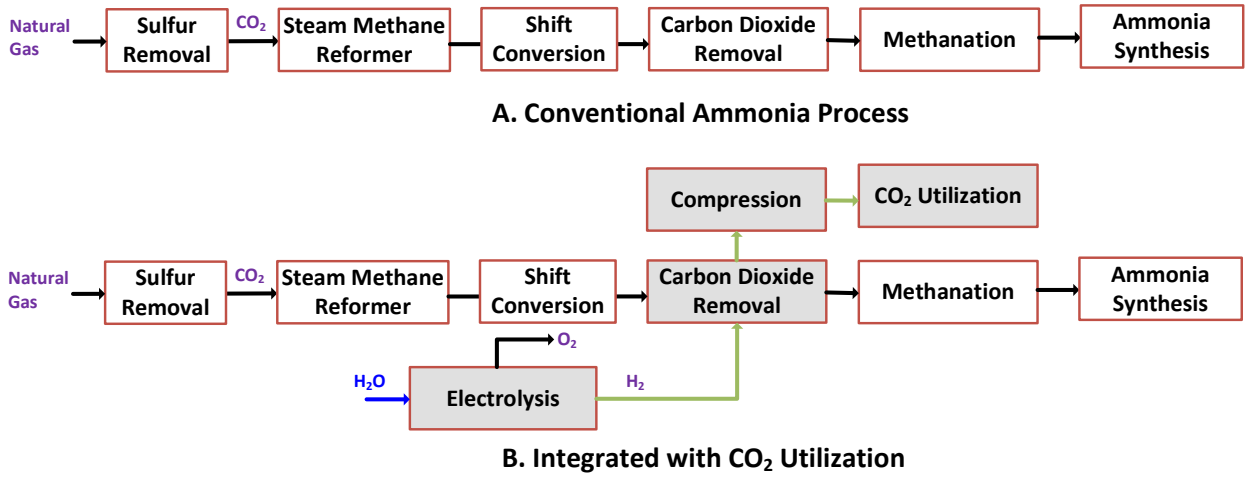

Figure 1. Simplified block diagram of the (a) Conventional ammonia production process, (b) Ammonia process integrated with the CO_2 utilization unit

In the CO_2 Utilization unit (Chapters 3.1 and 3.2), three different configurations for the DME production are investigated to define the best route with minimum CO_2 capture cost (Figure 2). The investigated pathways are:

a. Direct DME production: This one-step process involves the direct conversion of synthesis gas into dimethyl ether through a catalytic reaction. The reaction takes place using a dual catalyst system, where the first catalyst enables methanol synthesis and the second facilitates the subsequent dehydration of methanol to form DME.
b. Direct DME production with RWGS: In this pathway, the RWGS reaction is used in conjunction. This reaction is utilized to modify the composition of syngas by converting CO_2 into carbon monoxide CO and water H_2O before it enters the DME conversion stage.

c. Indirect DME production: This process involves a two-step process where methanol is first synthesized from syngas, and then methanol is subsequently dehydrated to produce DME.

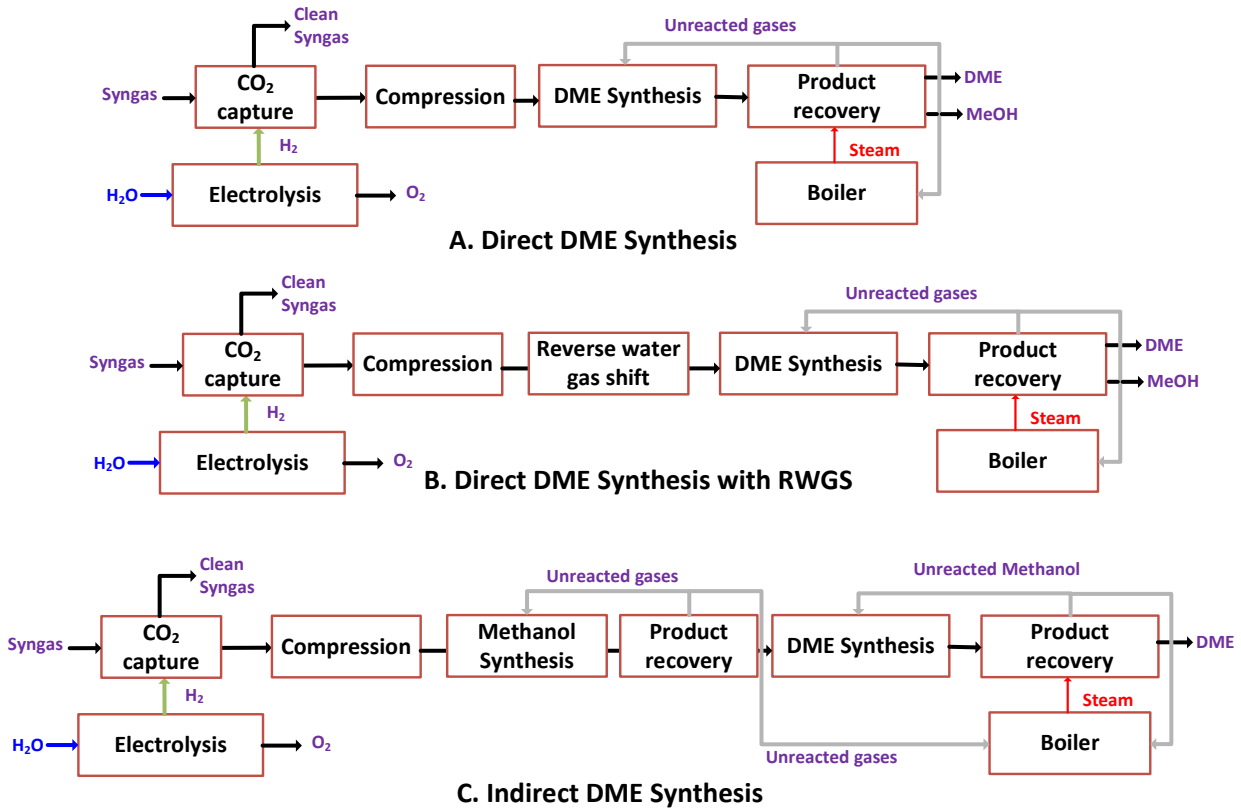

Figure 2. Simplified block diagram of the integrated CO_2 capture and utilization based on (a) Direct DME production, (b) Direct DME production with RWGS, and (c) Indirect DME production via methanol production

The process simulation of all routes is conducted using Aspen Plus® version 12.1 (Aspen Technology, Inc. Bedford, MA, USA). The Uniquac-RK thermodynamic model is used for all process units except for the CO_2 capture and steam generation boilers, where the Elec-NRTL and STEAMNBS methods are used for the Amine and steam generation units, respectively.

3.1. CO_2 Capture Unit

As mentioned earlier, the CO_2 Capture Unit is designed based on revamping an existing CO_2 capture process used for the syngas treatment of an ammonia plant. In the first step, the existing CO_2 capture based on amine solvent is simulated in Aspen Plus, and results are validated with the process data. Subsequently, the CO_2 capture unit is revamped by injecting hydrogen into the CO_2 regeneration column. The main purpose of injecting hydrogen is to reduce the temperature difference between the condenser and reboiler and incorporate an efficient low-pressure heat pump for effective electrification of the CO_2 capture unit.

The conventional CO_2 capture unit uses the Mono-Ethanol Amine (MEA) solvent for the CO_2 capture (Figure 3). The raw syngas stream, that it's composition comes from an example of an ammonia unit in Aspen Plus (Table 1), is sent to the high-pressure absorber column to be contacted with lean amine. The amine flowrate is adjusted to capture around 99.97% of the inlet CO_2 (raw syngas and recycled CO_2).

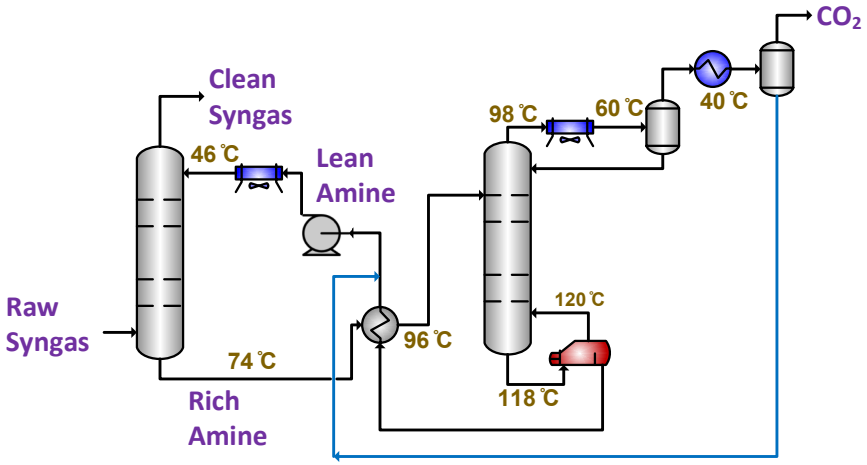

Figure 3. Schematic of the CO_2 Capture Unit using MEA solvent

Table 1. Raw syngas to the Amine unit

Flowrate, kg/h	100,187		
Temperature, °C	63	**Pressure, bar**	27.7
Composition, %wt			
CO_2	52	H_2O	1
N_2	37	CO	1
H_2	8		

The main reactions that occur in the absorber and regenerator are listed as follows.

$$2H_2O \leftrightarrow OH^- + H_3O^+ \quad (1)$$

$$H_2O + HCO_3^- \leftrightarrow CO_3^{--} + H_3O^+ \quad (2)$$

$$2H_2O + CO_2 \leftrightarrow HCO_3^- + H_3O^+ \quad (3)$$

$$H_2O + MEACOO^- \leftrightarrow MEA + HCO_3^- \quad (4)$$

$$H_2O + MEA^+ \leftrightarrow MEA + H_3O^+ \quad (5)$$

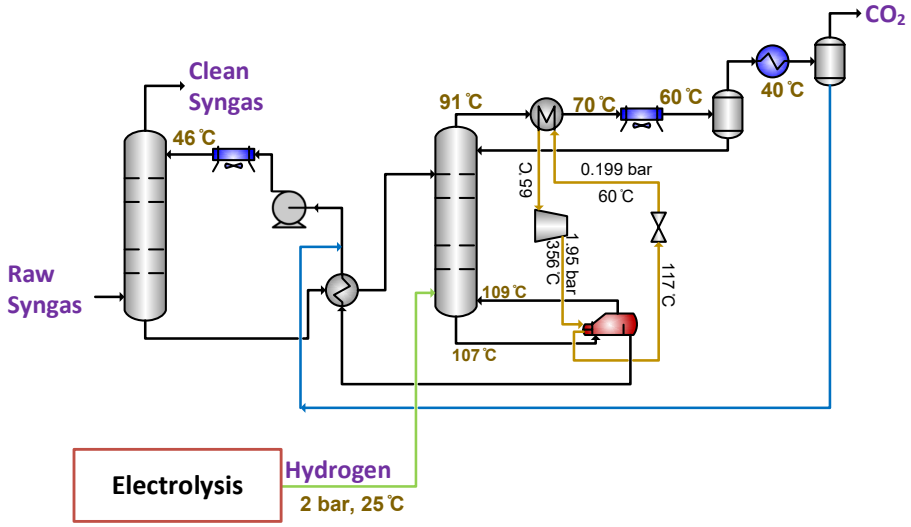

Figure 4. Schematic of the CO_2 Capture Unit with hydrogen injection and heat pump

In the modified CO_2 capture route (Figure 4), hydrogen is injected into the last stage of the CO_2 regeneration column. The hydrogen is sourced from a Proton Exchange Membrane (PEM), a technology that has been successfully commercialized for large-scale production, and is characterized by its compact design and rapid start-up capabilities [40,41]. The design parameters for the PEM have been taken from the study conducted by Colbertaldo et al. [41,42] and has operating conditions as 25 °C and 2 bar. The net energy demand of the unit is 52.37 kWh per kilogram of H_2 produced [43].

As it can be seen by comparing the temperature profile of both routes (Figure 3 and Figure 4), the hydrogen injection reduces the temperature profile of the reboiler and condensers. This lower temperature difference helps the heat pump that is used to supply the energy demand of the reboiler by the condenser, to achieve a relatively high coefficient of performance (COP) of 5.5. A low-pressure steam heat pump system is used, which provides low-pressure, high-temperature steam for the reboiler (356 °C), and then vaporized at 0.2 bar and 65 °C, in the condenser.

A summary of the process data and simulation results is shown Table 2. While the energy demands of the reboiler and condenser are around 4.6 and 1.6 (MJ/kg CO_2), respectively, the hydrogen injection into the amine unit integrated with the heat pump significantly reduced the energy demand. The new energy demands are 1.08 MJ/kg CO_2 for the reboiler and 2.49 MJ/kg CO_2 for the condenser.

Table 2. Process data and simulation results of the Amine unit

Absorber			
Number of stages	20	Top-stage pressure, bar	27.4
Regenerator			
Number of stages	19		
CO_2 capture, % of inlet (actual data)	99.9	CO_2 capture, % of inlet (simulation)	99.9
Condenser Duty (conventional), MJ/kg CO_2	19.66	Condenser Duty (simulation), MJ/kg CO_2	19.66
Reboiler Duty (conventional), MJ/kg CO_2	4.55	Reboiler Duty (simulation), MJ/kg CO_2	4.55
Condenser Duty (with heat pump), MJ/kg CO_2	2.49	Reboiler Duty (with heat pump), MJ/kg CO_2	1.08

3.2. CO_2 Compression Unit

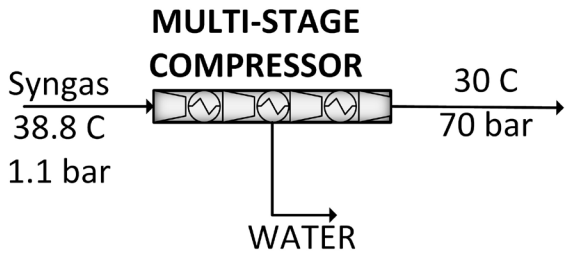

Figure 5. Schematic of the CO_2 Compression Unit

As can be appreciated in Figure 5, this unit is dedicated to the compression of captured carbon dioxide and hydrogen through a three-stage compression system with equal pressure ratio, and interstage cooling. This sequential compression process raises the gas pressure to 70 bar, alongside effecting the extraction of 99% of excess water.

3.3. Direct Method

As stated earlier, the direct method consists of the conversion of syngas directly into dimethyl ether. Two different scenarios are considered for the direct method: 1) without RWGS, and 2) with RWGS. In the first scenario, our baseline, the captured CO_2 and H_2 are directly sent to the DME reactor. However, due to the low conversion of CO_2, we also considered the second scenario, where CO_2 is first converted into CO using the Reverse Water Gas Shift reactor. The CO, CO_2, and H_2 mixture is then sent to the DME reactor.

3.3.1. Baseline (Direct Method)

Figure 6 shows the simplified process flow diagram of the direct method without RWGS.

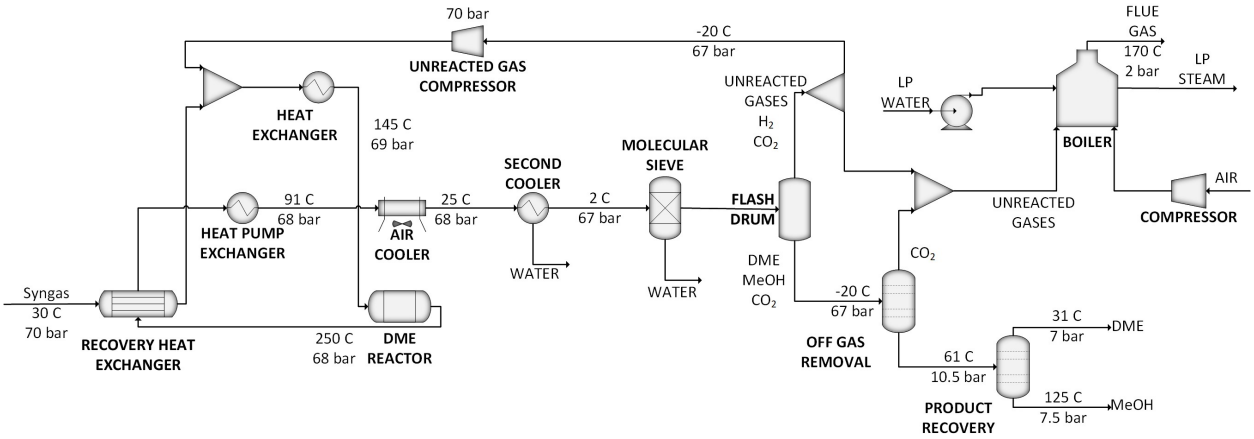

Figure 6. Process Flow Diagram of Direct Baseline Model

Details of the DME reactor and its catalyst conditions are presented in Table 5. The novel CuO-ZnO-ZrO_2@SAPO-11 core-shell catalyst is an initiative to produce more DME from syngas compared to a hybrid catalyst with the same composition [44], which involves the following reactions [45]:

$$CO + 2H_2 \leftrightarrow CH_3OH \quad (6)$$

$$CO_2 + 3H_2 \leftrightarrow CH_3OH + H_2O \quad (7)$$

$$CO_2 + H_2 \leftrightarrow CO + H_2O \quad (8)$$

$$2CH_3OH \leftrightarrow CH_3OCH_3 + H_2O \quad (9)$$

$$CO + 3H_2 \leftrightarrow CH_4 + H_2O \quad (10)$$

This is a bifunctional catalyst, where the CuO-ZnO-ZrO_2 is used as metallic function in the core, in which the synthesis of methanol and the RWGS reactions take place, while the acid function is achieved with SAPO-11 in the shell, where the methanol dehydration occurs [44]. The reaction rates, adsorption constants, and kinetic parameters are adopted from Ateka and Aguayo [45,46]:

$$r_{MeOH} = \left[k_1 \left(f_{H_2}^2 f_{CO} - \frac{f_{CH_3OH}}{K_1}\right) + k_4 \left(f_{H_2}^3 f_{CO_2} - \frac{f_{CH_3OH} f_{H_2O}}{K_4}\right)\right] \theta_{H_2O} \quad (11)$$

$$r_{DME} = k_2 \left[\left(f_{\mathrm{CH_3OH}}^2 - \frac{f_{\mathrm{CH_3OCH_3}} f_{\mathrm{H_2O}}}{K_2}\right)\right] \quad (12)$$

$$r_{WGS} = k_3 \left[\left(f_{\mathrm{H_2O}} f_{CO} - \frac{f_{\mathrm{CO_2}} f_{\mathrm{H_2}}}{K_3}\right)\right] \theta_{CO_2} \quad (13)$$

$$r_{HC} = k_5 \left[\left(f_{CO} f_{H_2}^3 - \frac{f_{HC} f_{\mathrm{H_2O}}}{K_3}\right)\right] \theta_{H_2O} \quad (14)$$

$$k_j = k_j^* exp\left[-\frac{E_j}{R}\left(\frac{1}{T} - \frac{1}{T^*}\right)\right] \quad (15)$$

$$K_{ads,i} = K_{ads,i}^* exp\left[\frac{\Delta H_{ads,i}}{R}\left(\frac{1}{T} - \frac{1}{T^*}\right)\right] \quad (16)$$

$$K_j = \exp\left(a + \frac{b}{T} + c \log T + dT + eT^2 + \frac{f}{T^2}\right) \quad (17)$$

$$\theta_i = \frac{1}{1 + f_i K_{ads,i}} \quad (18)$$

Where:

E: Activation energy, kJ mol^{-1}

f: Fugacity of component, bar

K_{ads}: Adsorption equilibrium constant, bar^{-1}

K: Equilibrium constant

k: Kinetic constant

T, T^*: Temperature and reference temperature, K

R: Universal gas constant, kJ/mol K

ΔH_{ads}: Adsorption heat, kJ mol^{-1}

θ: Term for quantifying the attenuation of the reaction rates by component

The corresponding equilibrium constant coefficients to be used with equation (17) have been documented by Aguayo and Ateka [39,46], which are listed in Table 3. Details regarding the kinetic parameters are provided in Table 4 [45].

Table 3. Coefficients of equilibrium constants of reactions equations (6), (8), (9) and (10) [39,46]

Reaction	**a**	**b**	**c**	**d**	**e**	**f**
Equation 6	21.84	9040	-7.66	0.005407	-5.75E-07	-6750
Equation 8	18.01	-5870	-1.86	0.000270	0	58200
Equation 9	-9.76	3200	1.07	-0.000660	4.90E-08	6050
Equation 10	24.9	22780	-7.95	0.004354	-3.61E-07	-4850

The coefficients pertaining to the reaction shown in equation (7), are calculated as the product of the reactions described in equations (6) and (8), since it is a linear combination of them.

Table 4. Kinetic parameters of CuO-ZnO-ZrO_2@SAPO-11 core-shell catalyst for DME production [45,46]

Parameter	**Value**	**Units**
k_1*	$1.71\ 10^{-5}$	$mol_{Methanol}\ g^{-1}\ h^{-1}\ bar^{-3}$
k_2*	$3.08\ 10^{1}$	$mol_{DME}\ g^{-1}\ h^{-1}\ bar^{-2}$
k_3*	$4.46\ 10^{1}$	$mol\ g^{-1}\ h^{-1}\ bar^{-2}$
k_4*	$9.23\ 10^{-7}$	$mol_{Methanol}\ g^{-1}\ h^{-1}\ bar^{-4}$
k_5*	$2.69\ 10^{-7}$	$mol_{H2}\ g^{-1}\ h^{-1}\ bar^{-4}$
E_1	$3.84\ 10^{0}$	$kJ\ mol^{-1}$
E_2	$2.31\ 10^{2}$	
E_3	$9.25\ 10^{1}$	
E_4	$8.82\ 10^{1}$	
E_5	205.35	
$K^*_{ads,H2O}$	$2.14\ 10^{0}$	bar^{-1}
$K^*_{ads,CO2}$	$1.15\ 10^{-1}$	
$\Delta H_{ads,H2O}$	$8.25\ 10^{-2}$	$kJ\ mol^{-1}$
$\Delta H_{ads,CO2}$	$1.61\ 10^{-1}$	
$K^*_{ads,H2O}$	$1.35\ 10^{-2}$	bar^{-1}
$K^*_{ads,CO2}$	$1.26\ 10^{-2}$	
$\Delta H^d_{ads,H2O}$	$1.02\ 10^{0}$	$kJ\ mol^{-1}$
$\Delta H^d_{ads,CO2}$	$9.70\ 10^{-1}$	

3.3.1.1. Reactor Design

In designing the DME reactor, a sensitivity analysis was conducted to maximize CO_2 conversion by varying reactor geometry, including length and number of tubes.

Table 5. Operating conditions of DME Reactor and Catalyst [45]

Reactor configuration	
Constant temperature (°C)	250
Inlet pressure (bar)	70
Number of tubes	10000
Length (m)	4.2
Diameter (cm)	4
Heat duty (kW)	0
Pressure drop correlation	Ergun
Catalyst condition	
Bed voidage	0.4
Particle density (g/cm^3)	0.615
Diameter (mm)	1
Shape factor	1

The captured and compressed carbon dioxide accompanied with hydrogen to 70 bar is preheated using the recovery heat exchanger, which is heated with the stream coming out of the reactor to create a heat recovery loop. The mixture is then combined with unreacted gases from a later stage of the process, creating a feed that is rich in mainly H_2 and CO_2. Next, the feed is preheated to 145.2 °C using a heat exchanger and sent to the DME reactor. This heater ensures the reactor remains adiabatic and avoids the need for additional heat at the reactor temperature. The specific temperature is calculated based on a design specification, changing the temperature of the heater before the reactor, so the heat demand of the later is 0 (Adiabatic reactor). The H_2/CO_X ratio of the feed stream is approximately 2.9, where CO_X is a mixture of CO and CO_2. The operating conditions of the DME reactor are based on those adopted from Ateka [45].

An evaluation was conducted through a sensitivity analysis to determine the influence of reactor temperature on the DME production rate (kg/h) over the CO_2 (kg/h) that comes as feed. The results, displayed in Figure 7, indicate that our design is most efficient at 250 °C. It is worth mentioning

that the catalyst's kinetics have only been verified within the range of 250 – 325 °C, and thus, lower temperatures were not considered.

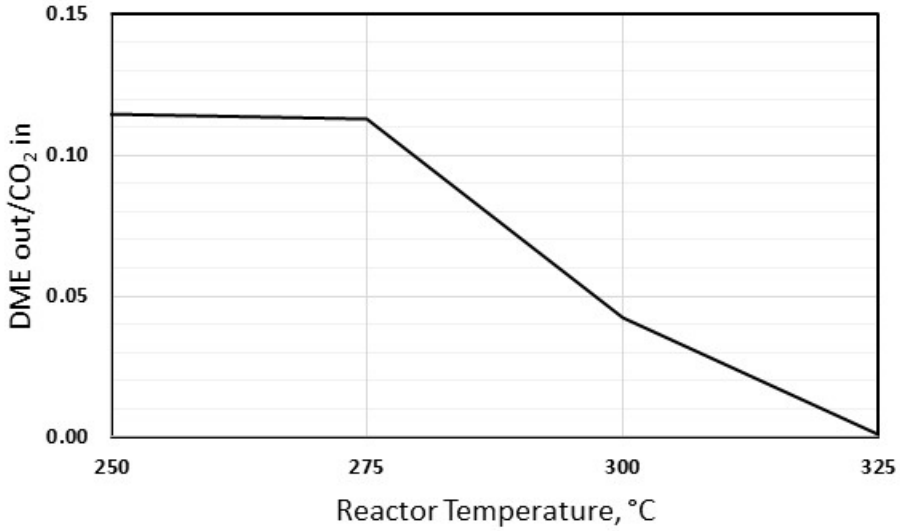

Figure 7. Impact of the DME reactor temperature and DME produced/inlet CO_2 ratio

The reactor length was set to 4.2 [45], and then a sensitivity analysis was conducted to evaluate the impact of the number of tubes on the production rate in kg/h of DME over the kg/h of CO_2 that is used, and the pressure drop in bar, the results are presented in Figure 8.

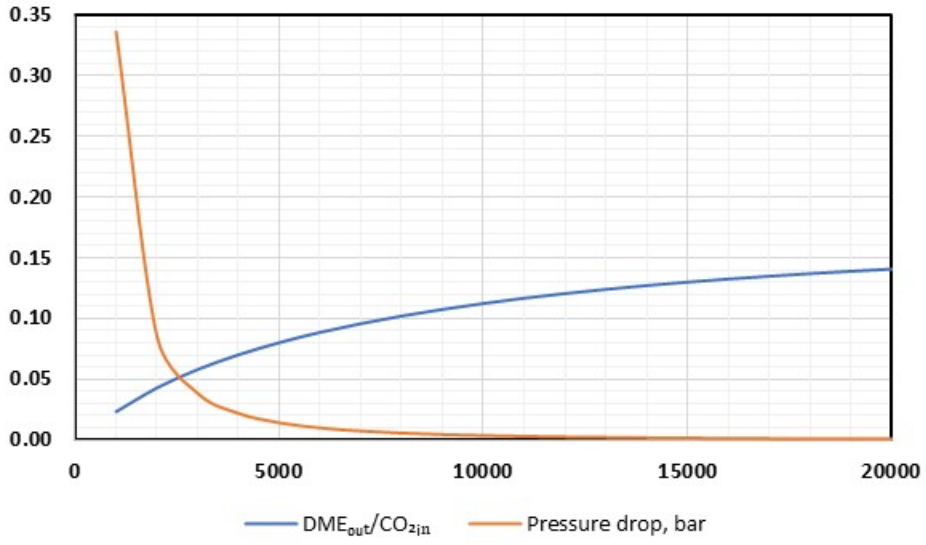

Figure 8. Sensitivity analysis of DME reactor for number of tubes vs DME produced/CO_2 in the feed and pressure drop

This analysis sheds light on how the production rate of DME is affected by the number of tubes used in the reactor. With 10000 tubes, a DME to CO_2 ratio of 0.11 is achieved, while 20000 tubes result in a ratio of 0.14 - a 25% increase, despite the doubled size. In an effort to be more realistic and avoid an oversized reactor, the number of tubes was restricted to 10000. The pressure drop experiences a slight decrease with more tubes, starting at 0.35 bar and becoming insignificant at around 3000 tubes, reaching nearly 0.01 bar.

3.3.1.2. Product Recovery

In the design of this process, we have accounted for a standard pressure drop of 0.5 bar across all equipment. After exiting the reactor, and going through the countercurrent heat exchanger, for heat recovery purposes, the feed undergoes a series of cooling and purification steps. Initially, the feed was cooled using the heat pump exchanger, primarily intended to supply heat deficit in the CO_2 capture unit's heat pump, which is already discussed in detail in the CO_2 capture section. The heat pump requires 59.75 Gcal/h to vaporize its fluid (water). The stripper's condenser supplies 30.59 Gcal/h of the required heat, and the remaining part is provided by this exchanger.

Following this, the cooled feed is sent to an air cooler which lowers the temperature to 25 °C, and afterwards a second cooler that decreases the temperature to 2 °C. In this latter cooler, approximately 99.6% of its water is removed.

Further in the process, the feed passes through a molecular sieve equipped with a desiccant type 3A. This sieve has the capacity to adsorb up to 20% of its weight in water, effectively eliminating the remaining water content from the feed [47].

Subsequently, the flow is directed to a flash drum operating at a temperature of -20 °C to segregate the unreacted gases from the desired product. The unreacted gases are then redirected back for recycling, with a reflux ratio of 97%, before being subjected to a compressor with isentropic efficiency of 72% to reach a pressure of 70 bar. This enables the mixture to be blended with the fresh inlet stream and reintroduced into the reactor. The residual 3% of the vapor phase is sent to the boiler as the purge gas stream.

3.3.1.3. Distillation Columns

To create the desired final products, the DME-rich liquid stream undergoes a two-step process involving distillation columns. The off gas removal distillation column, which features a 30-stage setup with a reflux ratio of 7.9 and a boilup ratio of 2.8, produces a liquid stream rich in 0.33 mole fraction of MeOH and 0.67 of DME, and a vapor stream rich in CO_2, with a mole fraction of 0.77, followed by 0.17 mole fraction of CH_4 and other unreacted gases. The resulting vapor phase is then directed to the boiler. The selection of reflux and boilup ratios is based on two design specifications: the first one aims for a 0.99 mass recovery of DME in the bottom stream, while the second targets a 0.99 mass recovery of CO_2 in the top stream.

The Product recovery distillation column uses a 30-stage column with a specific reflux ratio of 0.1 and boilup ratio of 1.2, as per the design specifications required to attain the desired mass purity and mass recovery of the end products. This process results in a final product recovery rate of 99.9% for each stream, with DME achieving a purity level of 98.5% [48] and MeOH reaching a purity level of 99.85% [49].

Table 6. Operation conditions for distillation columns of direct model

	1st - Off Gas Removal	**2nd - Product Recovery**
Stages	30	30
Feed stage	25	25
Reflux ratio	7.9	0.2
Boilup ratio	2.8	1.2
Condenser pressure (bar)	10	7
Column pressure drop (bar)	0.5	0.5
Design spec 1	DME mass recovery: 0.99	DME mass purity: 0.985
Design spec 2	CO_2 mass recovery: 0.99	DME mass recovery: 0.9995

3.3.1.4. Heat Demand

The DME Unit supplies the heat demand of the entire process by utilizing unreacted vapor phase feeds that are rich in H_2 and CH_4, which come from the flash separator and off gas removal distillation column. These feeds are sent to an adiabatic boiler (since no energy is not being transferred with the environment), where they are burned with compressed air at a pressure of 2

bar. The flow rate of air is carefully adjusted to ensure optimal combustion, resulting in flue gas that contains an excess 10% of O_2, therefore guaranteeing complete combustion. The flue gas stream exiting the boiler has a minimum temperature of 170 °C, to be above the acid dew point and avoid any acid condensation [50]. In this boiler, the heat is exchanged with a stream of low-pressure water. The flow rate of the water is determined by another design specification to ensure that the saturated steam leaving the heat exchanger can provide enough heat for other equipment such as heat exchangers and distillation columns.

3.3.1.5. Refrigeration Duty

There are three pieces of equipment that require extremely low temperatures: the second cooler, the flash separator, and the condenser of the off-gas removal distillation column. A three-stage propane refrigeration cycle is used for all refrigeration duties. The correlation proposed by A. Bahadori [51] is used to calculate the compressor power and condenser duty per refrigeration duty of the refrigerant system. By using this correlation and taking into consideration that the system requires a refrigeration temperature of approximately -30 °C, assuming a refrigeration condensing temperature of 25 °C, we were able to determine that for every MW of refrigeration duties, 375 kW of power were required.

3.3.2. Modified (Direct Method with RWGS)

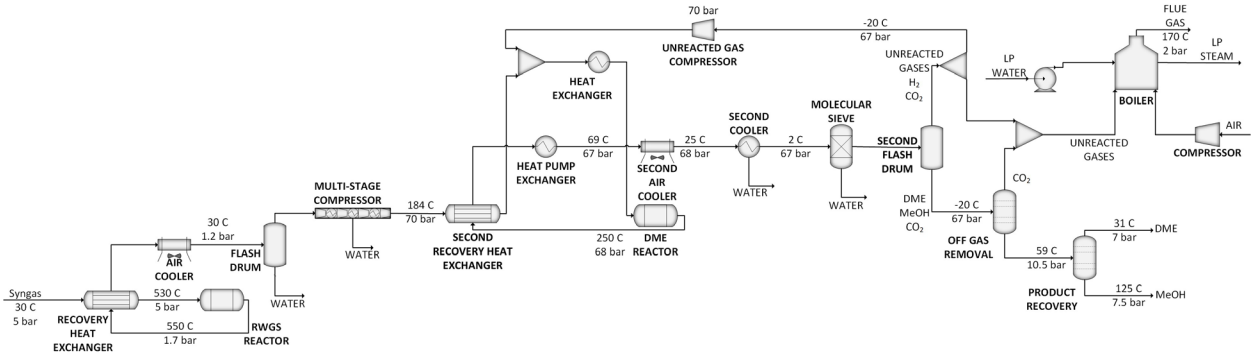

Figure 9. Process Flow Diagram of Direct Modified Model with RWGS

The Direct Method modified with RWGS (Figure 9) has similar process units and operating conditions for the majority of its equipment, as the Direct Method. These conditions encompass parameters like temperature, pressure, and feedstock composition, which serve as the common framework for both methods. However, our attention in this method is directed towards elucidating the key distinctions that set the RWGS in the process.

During our search for the optimal kinetics for this reaction, we explored various sources. Initially, we tested the kinetics proposed by Yongtaek et al. for WGS [52]. As the reaction is reversible and the catalyst used was $CuO/ZnO/Al_2O_3$, we adjusted the kinetics accordingly, utilizing their empirical rate expression derived from testing different models. Additionally, we looked into the kinetics suggested by Z. Yichen [32], which involved using ruthenium-modified catalysts at different %wt modifications, all operating at the same desired temperature conditions. Ultimately, we found that the kinetic described by S. Dzurik et al. [33] produced the most reasonable results that could be supported by experimental data.

The reaction taking place is reported on equation (8): $CO_2 + H_2 \leftrightarrow CO + H_2O$ and kinetics are taken from S. Dzurik et al. [33]. The details of the reactor and its catalyst are summarized in Table 7. The reactor is designed to operate at high temperatures, and to achieve that, it requires a reliable heating source. The electric heater, with an efficiency of 95% [53], is employed to provide the required heat energy for the reactor to function optimally.

Table 7. Operating conditions of RWGS Reactor and Catalyst [33]

Reactor configuration	
Constant temperature (°C)	550
Inlet pressure (bar)	5
Number of tubes	200
Length (m)	1
Diameter (cm)	4
Heat duty (kW)	7348
Pressure drop correlation	Ergun
Catalyst condition	
Bed voidage	0.55
Particle density (g/cm^3)	5.904

Diameter (mm)	1
Shape factor	1

The reactor of the unit is a packed-bed with 1 m of length, given that the reaction rate approaches zero within the first 0.5 m of the reactor entrance [33]. Based on the pressure drop of 3.2 bar in this configuration, we have set the number of tubes to 200. However, it is important to note that increasing the number of tubes does not have a significant effect on the conversion of CO_2 into CO. The critical factor that influences the conversion rate is the reactor temperature, which is set be 550 °C to achieve a CO_2 conversion of 54%. The kinetic model results are compared with the equilibrium conversion and shown in Figure 10.

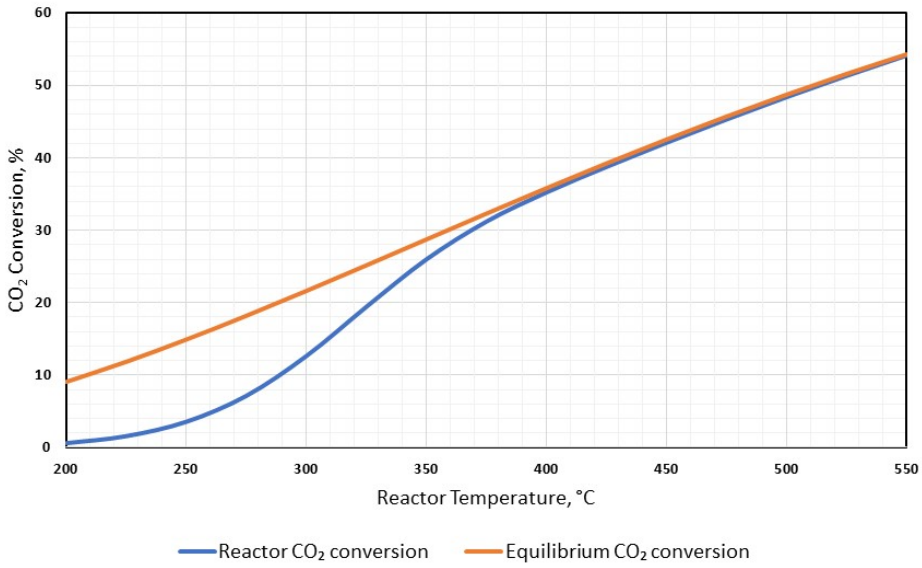

Figure 10. Conversion of CO_2 in $CuO/ZnO/Al_2O_3$ catalyst reactor and equilibrium vs temperature

The power law reaction rate of the RWGS reaction over the $CuO/ZnO/Al_2O_3$ catalyst is described in the following equations [33]:

$$r = k_o e^{-\left(\frac{E_a}{R_g T}\right)} \left(y_{CO_2} y_{H_2} - \frac{y_{CO} y_{H_2O}}{K_{eq}}\right) C_{FP} \quad (19)$$

$$C_{FP} = \frac{P^{0.5-(P/25000000)}}{100000} \quad (20)$$

$$K_{eq} = e^{4.33-(4577.8/T)} \quad (21)$$

Where:

T: Temperature, K

P: Pressure, Pa

y: Mole fraction

k_o: Pre-exponential constant, mol/kg_{cat} s

E_a: Activation energy, J/mol

C_{FP}: Pressure correction factor

Table 8. Kinetic parameters of $CuO/ZnO/Al_2O_3$ catalyst for CO production [33]

Parameter	Value	Units
k_o	$2.1852\ 10^5$	mol/kg_{cat} s
E_a	$7.1623\ 10^4$	J/mol

3.3.2.1. Reactor Design

As mentioned earlier, the RWGS reaction occurs in the packed-bed reactor filled with the $CuO/ZnO/Al_2O_3$ catalyst under conditions of 5 bar and at a constant temperature of 530 °C. The operating conditions are adjusted to achieve a H_2/CO_X ratio of 2 to 3, and a CO_2 conversion of around 54%. Subsequently, the reactor outlet, after heat recovery is sent to an air cooler to attain an ambient temperature of 30 °C. Following this cooling stage, the stream is sent to the flash separator to remove the 76% excess water generated in the reactor in liquid phase and it from the gas stream. The processed gas stream is subsequently subjected to a four-stage isentropic compression, increasing its pressure to 70 bar while concurrently extracting 95% additional water. Following this step, the process operates similarly to the baseline model.

3.4. Indirect

The indirect method for transforming syngas into DME entails a two-step process. Initially, methanol (MeOH) is produced by converting CO_2, followed by a subsequent conversion of MeOH into DME. The catalytic conversion of CO_2 to MeOH is conducted using a traditional Lurgi two-stage model that was not subject to modification in this thesis. The production of DME relies on MeOH dehydration, and we will delve into each process unit in the subsequent sections.

3.4.1. MeOH Production Unit

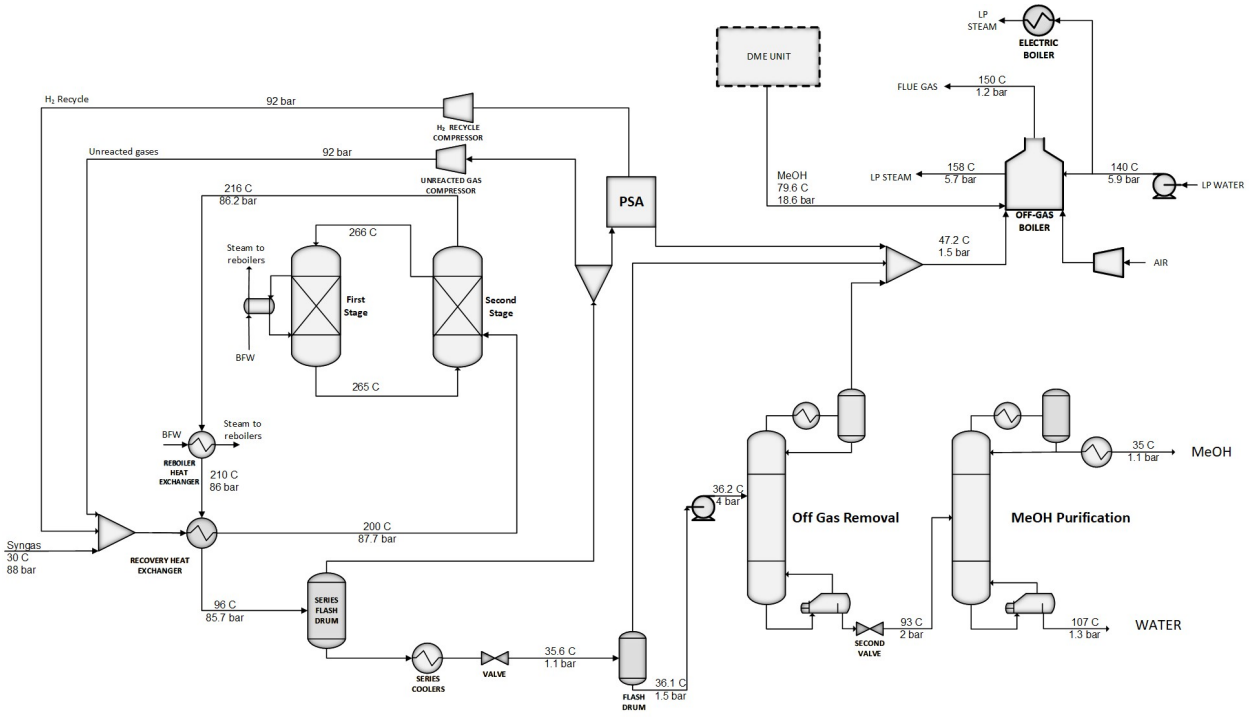

Figure 11. Process Flow Diagram of Indirect Model; MeOH Unit

For this reaction we used a $CuO/ZnO/Al_2O_3$ catalyst, in the previously mentioned two-stage Lurgi reactor, which is widely used in this type of process. The reactions involved in this process are the ones previously mentioned in equations (8), (7), and (9), as well as the following equation:

$$2CO + 4H_2 \leftrightarrow C_2H_6O + H_2O \quad (22)$$

They were adapted from Vanden Bussche et al. [54]. Table 9 contains the information regarding the MeOH reactor and its catalyst.

Table 9. Operating conditions of MeOH Reactor and Catalyst

Reactor configuration		
	First Stage	**Second Stage**
Reactor type	Reactor with constant thermal fluid temperature	
Heat transfer (cal/s cm^2 K)	0.22	0.83
Thermal fluid temperature (°C)	265	267
Inlet pressure (bar)	87.66	86.46
Number of tubes	5095	1
Length (m)	5	4.1
Diameter (m)	0.04	3.98
Heat duty (kW)	-13787	-18954
Pressure drop correlation	Ergun	Ergun
Catalyst condition		
Bed voidage	0.35	0.35
Particle density (g/cm^3)	1.94	1.94
Diameter (mm)	6	6
Shape factor	1	1

The rate constants of the equations previously mentioned are [55]:

$$r_{MeOH} = \frac{k_1 P_{CO_2} P_{H_2} - k_2 P_{H_2O} P_{MeOH} P_{H_2}^{-2}}{(1 + k_3 P_{H_2O} P_{H_2}^{-1} + k_4 P_{H_2}^{0.5} + k_5 P_{H_2O})^3} \quad (23)$$

$$r_{RWGS} = \frac{k_6 P_{CO_2} - k_7 P_{H_2O} P_{CO} P_{H_2}^{-1}}{(1 + k_3 P_{H_2O} P_{H_2}^{-1} + k_4 P_{H_2}^{0.5} + k_5 P_{H_2O})^3} \quad (24)$$

$$r_{ETOH} = K_{ETOH} P_{CO} P_{H_2}^{1.5} (W_{cat} F_{cat}) \quad (25)$$

$$r_{DME} = K_{DME} P_{MeOH}^2 (W_{cat} F_{cat}) \quad (26)$$

The kinetic constants of ethanol and dimethyl ether are calculated using the equation (27), where the reference temperature T_0 is 228.42 °C, and the kinetic values are presented in Table 10 [55].

$$K_i = K_{o,i} \exp\left(-\frac{E_i}{R}\left(\frac{1}{T} - \frac{1}{T_0}\right)\right) \quad (27)$$

Table 10. Equilibrium constant and activation energy for ETOH and DME production rate [55]

Kinetic values	Ethanol	Dimethyl Ether	Units
$K_{o,i}$	1.00E− 12	4.20E− 11	mol/kg_{cat} s
E_i	19.47	18.66	kcal/mol K

To calculate the kinetic constants for the rest of the reactions, we used the equation (28) as mentioned by Barati et al. [55]. Using the kinetic values described in Table 11.

$$lnk_i = A_i + \frac{B_i}{T} \quad (28)$$

Table 11. Kinetic values for MeOH and RWGS production rate [55]

Kinetic constant	A_i	B_i (k)
k_1	-29.87	4811.16
k_2	17.55	-2249.8
k_3	8.15	0.00
k_4	6.45	2068.44
k_5	-23.44	14928.92

Where:

T: Temperature, K

k: Kinetic constant

K: Equilibrium constant

P: Partial pressure, bar

W_{cat}: Weight of catalyst, kg

F_{cat}: Activity of catalyst

R: Universal gas constant, kJ/mol K

E: Activation energy, kcal/mol K

The process starts by introducing syngas to the system under specific conditions: a temperature of 30 °C and a pressure of 88 bar. The syngas is then combined with recycled H_2 and unreacted gases. The mixture is heated to 200 °C via a heat exchanger before being subjected to further heating using the tube side of the second reactor, raising the temperature to 266 °C. In the first reactor, the

mixture flows through catalyst-packed tubes, where the reactions take place. In the second stage, the mixture flows through the packed shell of the reactor while the incoming syngas, flowing counter-current through the tubes, contributes to lowering the temperature.

The feed is then cooled down to 210 °C with the reboiler heat exchanger, which purpose is to provide heat for steam production for the reboiler. Subsequently it is cooled down to 96 °C with the recovery heat exchanger. To prepare the feed for the next stage, it undergoes a series separation stages, using flash drums, coolers and a valve, ultimately reaching a temperature of 35.6 °C. This purification process is critical to eliminate any remaining H_2 and CO_2 from the feed. Ultimately, a 0.99 split fraction of the resulting unreacted gas mix from this purification stage is recycled back, after being pressurized to 92 bar, and mixed with the clean syngas that comes from the CO_2 Capture/CO_2 Compression units. The remaining 0.01 fraction of the gas mix is sent to a PSA (Pressure Swing Adsorption) process [56], where 86% of the hydrogen is recovered. This gas mix contains 0.95 mole fraction of H_2, that is later recycled to be mixed with the clean syngas, going first through a compressor that increases the pressure of the feed to 92 bar [43]. The remaining 14% of the hydrogen is sent to the boiler for heat recovery.

After the purification stage of the stream, we obtained a liquid stream rich in MeOH with presence of water, with a mole fraction of 0.49 each. It is then pressurised with the pump to 4 bar, and sent to the off gas removal distillation column, which conditions are described in Table 12. This first distillation column separates the carbon dioxide from the feed, and this carbon dioxide is later sent to the boiler. The liquid stream rich in MeOH and water, is sent to the MeOH purification distillation column (conditions described in Table 12) achieving a 99.85% of purity of MeOH [49].

Table 12. Operation conditions for distillation columns of MeOH unit in the indirect model

	1st - Off Gas Removal	**2nd - MeOH Recovery**
Stages	30	45
Feed stage	2	15
Reflux ratio	0.03	1.50
Boilup ratio	0.23	1.99
Condenser pressure (bar)	2.5	1.06
Column pressure drop (bar)	0.5	0.3
Design spec 1	MeOH mass recovery: 0.99	MeOH mass purity: 0.9985
Design spec 2	CO_2 mass recovery: 0.995	MeOH mass recovery: 0.99

3.4.1.1. Heat Demand

In this section, we delve into the heat integration system of the MeOH unit. Initially, heat from the first stage of the MeOH reactor is extracted and utilized for producing low-pressure steam. The resulting steam is then utilized to supply the heat demand of reboilers. Additionally, the steam produced by using the heat that comes from the first stage of the MeOH and immediately after the second stage of the MeOH reactor, are used for heat integration in the reboiler.

The additional heat demand of the distillation columns of the MeOH and DME units are supplied by generating low-pressure steam from purged gases, which are combusted with air in the boiler. To optimize the heat recovery, the amount of water sent to the boiler is calculated to cool the flue gas to the acid dew point. Any additional heat demand is supplied by an electric heater with 95% efficiency [53]. The heat of the steam produced is sent to the reboiler for heat recovery.

3.4.2. DME Production Unit

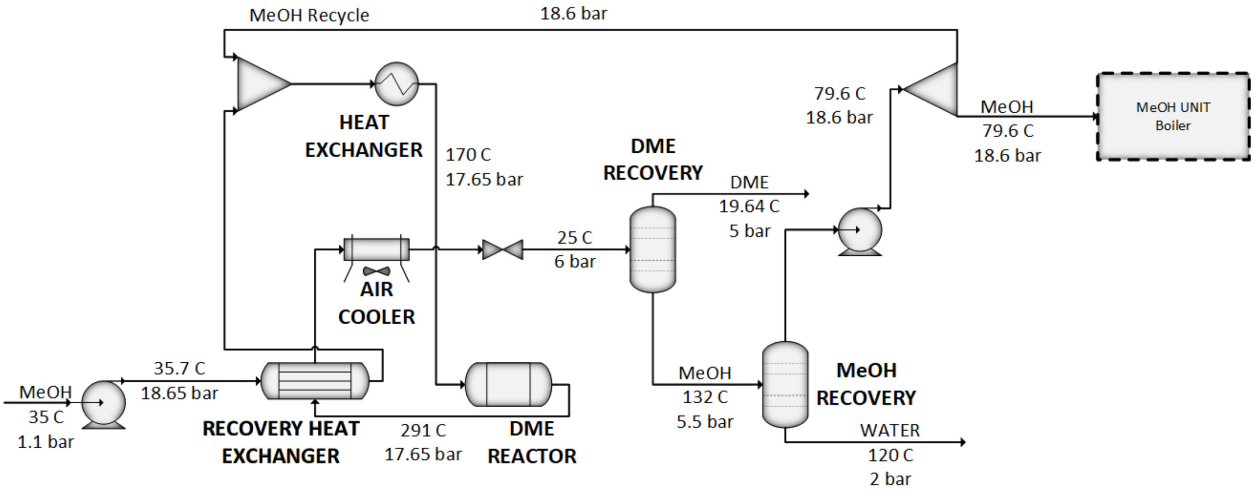

Figure 12. Process Flow Diagram of Indirect Model; DME Unit

The process of conversion of MeOH into DME is done through a ɣ-Al_2O_3 catalyst. The reaction detailed in equation (9): $2CH_3OH \leftrightarrow CH_3OCH_3 + H_2O$, occurs in a fixed-bed adiabatic reactor operating at 291 °C and 17.65 bar. The details of the reactor and catalyst are described in Table 13.

Table 13. Operating conditions of DME Reactor and Catalyst Indirect [57]

Reactor configuration	
Reactor type	Adiabatic
Maximum temperature (°C)	291
Inlet pressure (bar)	17.65
Number of tubes	1
Length (m)	8
Diameter (m)	3.8
Heat duty (kW)	0
Pressure drop correlation	Ergun
Catalyst condition	
Bed voidage	0.5
Particle density (g/cm^3)	2.01
Diameter (mm)	1
Shape factor	1

To ensure optimal fluid velocity inside the industrial DME reactor via MeOH dehydration, the reactor's size was determined based on the recommendation of Dimian et al. to achieve a velocity of approximately 0.25 m/s [57]. A sensitivity analysis was conducted to select the inlet feed temperature, evaluating a range of temperatures from 160 to 400 °C against the DME production rate (kg/h) over the MeOH (kg/h) from the previous unit without recycle stream. As the reaction cannot occur below 160 °C, the operating temperature was set at 170 °C, resulting in a ratio of 0.62, as illustrated in Figure 13, following the approach of Mollavali et al. [58].

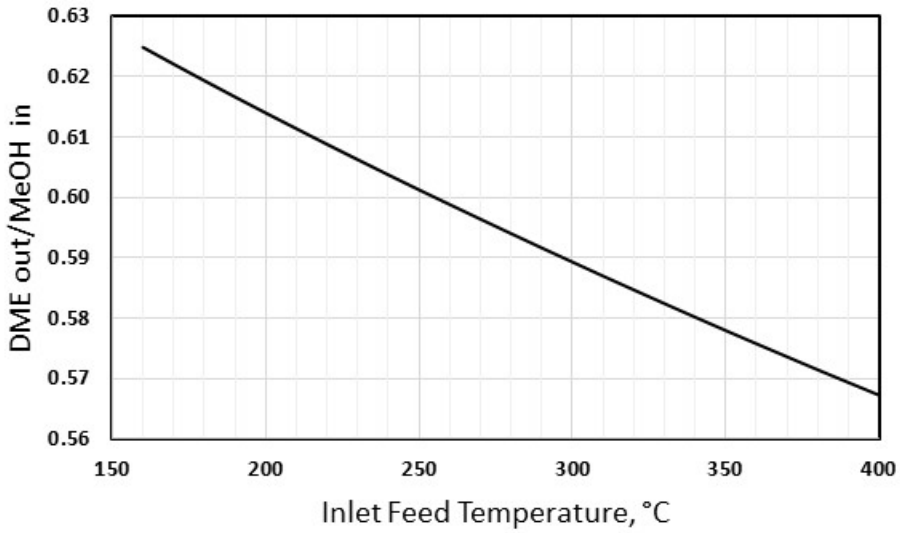

Figure 13. Sensitivity analysis of DME reactor for inlet feed temperature versus DME out/MeOH in

The kinetics for this reaction are adapted from Mollavali et al. [58], as they tested it with the same catalyst and similar conditions of temperature and pressure. The equilibrium constant was computed from Gibbs energies by Aspen Plus.

$$r = \frac{kK_m^2\left(P_m^2 - \frac{P_w P_d}{K_{eq}}\right)}{\left(1+2\sqrt{K_m P_m}+K_w P_w\right)^4} \quad (29)$$

$$k = 3.3\ 10^9 \exp\left(-\frac{10800}{T}\right) \quad (30)$$

$$K_m = 0.72\ 10^{-2} \exp\left(\frac{830}{T}\right) \quad (31)$$

$$K_w = 0.45\ 10^{-2} \exp\left(\frac{1130}{T}\right) \quad (32)$$

Where:

k: Rate constant of reaction, kmol/kg_{cat} h

K_m: Adsorption constant methanol

K_w: Adsorption constant water

K_{eq}: Equilibrium constant

P: Partial pressure, bar

T: Temperature, C

3.4.2.1. Reactor Design

As shown in Figure 12, the liquid MeOH, which was previously obtained from the unit at 35°C, is pressurized to 18.65 bar using a pump. Following this, it flows through the heat recovery exchanger, where the heat from the product stream coming out of the reactor is employed. The resultant mixture is then combined with unreacted MeOH liquid, which is recycled back. Finally, the mixture is heated to a temperature of 170 °C with an electric heater at 95% efficiency [53]. In the reactor, a MeOH conversion rate of 87% was successfully achieved, turning it into 72% dimethyl ether and 28% water. The product stream is cooled down through the recovery heat exchanger and the air cooler. Its pressure is then reduced by a valve, resulting in conditions of 25°C and 6 bar.

3.4.2.2. Distillation Columns

This DME is then retrieved with the product recovery distillation column, where water, methanol and ethanol are separated from the feed and sent to the bottoms, giving a stream of DME at 98.5% purity [48]. The bottom liquid stream with the unreacted methanol, is sent to the MeOH Recovery distillation column, removing 97% of the water and recovering 99.5% of the MeOH in the stream for recycling. The specifications of these two columns are described in Table 14.

Table 14. Operation conditions for distillation columns of DME unit in the indirect model

	1st - Product Recovery	**2nd – MeOH Recovery**
Stages	30	15
Feed stage	25	10
Reflux ratio	0.38	2.00
Boilup ratio	0.91	1.03
Condenser pressure (bar)	5	1.5
Column pressure drop (bar)	0.5	0.5
Design spec 1	DME mass purity: 0.985	MeOH mass recovery: 0.995
Design spec 2	DME mass recovery: 0.9995	

The recovered MeOH is then pressurized again with a pump and divided, 0.99 of it is sent back to be mixed with the feed of MeOH, and 0.01 is sent to the boiler of the MeOH Unit previously described.

4. Results and Evaluation

With the three pathways described in detail, now we can address the results of the simulations. DME and MeOH are considered as the product and byproduct respectively. The three processes are going to be addressed in each section, as comparison facilitates a comprehensive evaluation of each pathway. Summarized details of the results are available in Table 15.

Table 15. Overall mass balance and energy demand of pathways

	Direct	**Direct with RWGS**	**Indirect**
CO_2 in (kg/h)	52113	52113	52113
CO_2 out (kg/h)	10487	6833	3246
DME out (kg/h)	16229	19103	25040
MeOH out (kg/h)	7367	6055	0
Energy demand (MW)	573	586	616

4.1. Production Results

First, we will assess the efficiency of three techniques in regard to their output in kilograms per hour. The Direct Method exhibited a DME production of 16,229 kg/h, accompanied by a MeOH byproduct of 7,367 kg/h. This data emphasizes a notable disparity, with the primary target product DME constituting roughly 69% of the overall yield, while the unintended byproduct MeOH makes up the remaining 31%.

The Direct Method, when combined with RWGS, resulted in a total production amounting to 19,103 kg/h of DME. This represents a significant 18% increase in yield as compared to the baseline. Correspondingly, there was a 18% decrease in MeOH production, bringing the total to 6,055 kg/h. In this particular pathway, DME accounted for 76% of the total products, while MeOH accounted for the remaining 24%. It is worth to note that the modified RWGS method exhibited an overall 7% increase in fuel production as compared to the baseline method.

The Indirect Method exhibited an absence of byproduct, obtaining solely as total production 25,040 kg/h of DME. This outcome means an increase in production by 54% concerning the established baseline, and 31% compared with the modified pathway with RWGS, as can be seen in Figure 14.

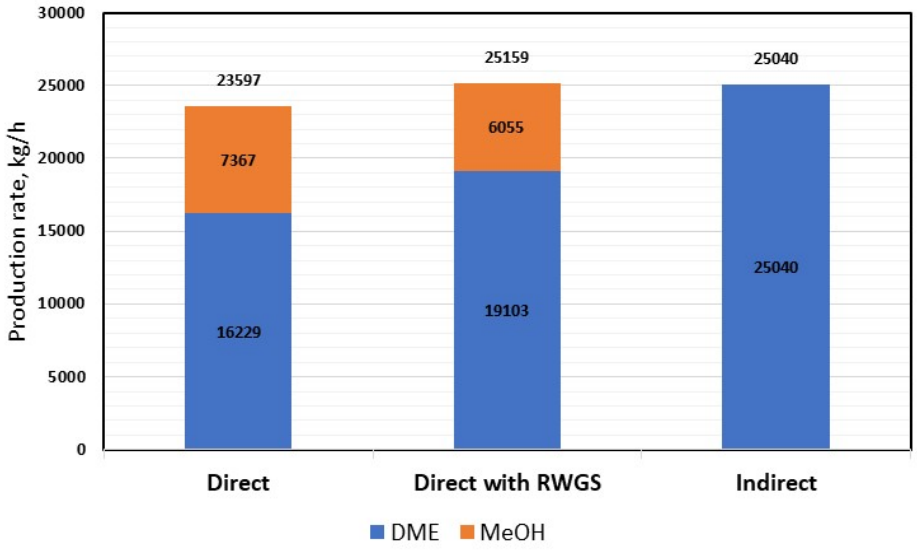

Figure 14. Production rate of pathways

4.2. CO_2 Utilization

The results of the carbon dioxide utilization rate for each pathway are shown in this section. As it is shown in Figure 15, the Direct Method initially stands out, having a CO_2 utilization rate of 1.21 kg CO_2/kg DME and 0.55 kg CO_2/kg MeOH. Upon modification with the incorporation of the RWGS in the process, the Direct Method exhibits a slight increase in CO_2 utilization rate, measuring at 1.37 kg CO_2/kg DME and 0.43 kgCO_2/kgMeOH. In contrast, the Indirect Method records a comparatively higher CO_2 utilization rate of 1.95 kg CO_2/kg DME.

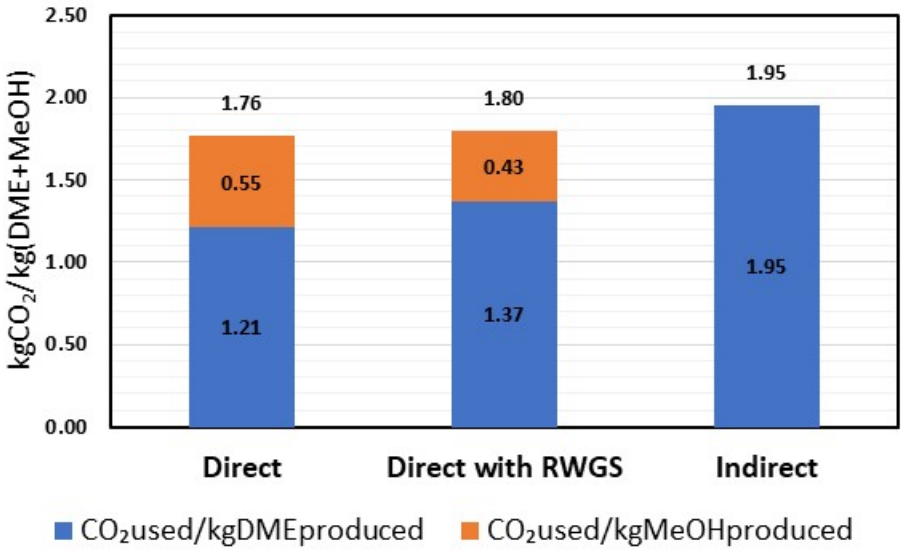

Figure 15. Carbon dioxide utilization of pathways

This observation elucidates a reduction in the residual amount of unused and purged CO_2 in the Indirect pathway. Consequently, for the same quantity of CO_2 utilized across the various pathways, a higher yield of DME is obtained.

4.3. Hydrogen Consumption

The distribution of hydrogen use across the various routes shows significant differences. The cumulative hydrogen consumption in the Direct approach is 0.288 kg of hydrogen per kg of DME and MeOH. In contrast, the pathway employing the Direct Method but modified with the integration of the RWGS process reflects a slightly diminished hydrogen consumption, 0.270 kg of hydrogen per kg of (DME+MeOH), which means a more optimized allocation of hydrogen towards the desired product. Furthermore, the Indirect method achieves a hydrogen consumption rate of 0.271 kilograms of hydrogen per kilogram of DME produced. This can be observed in Figure 16.

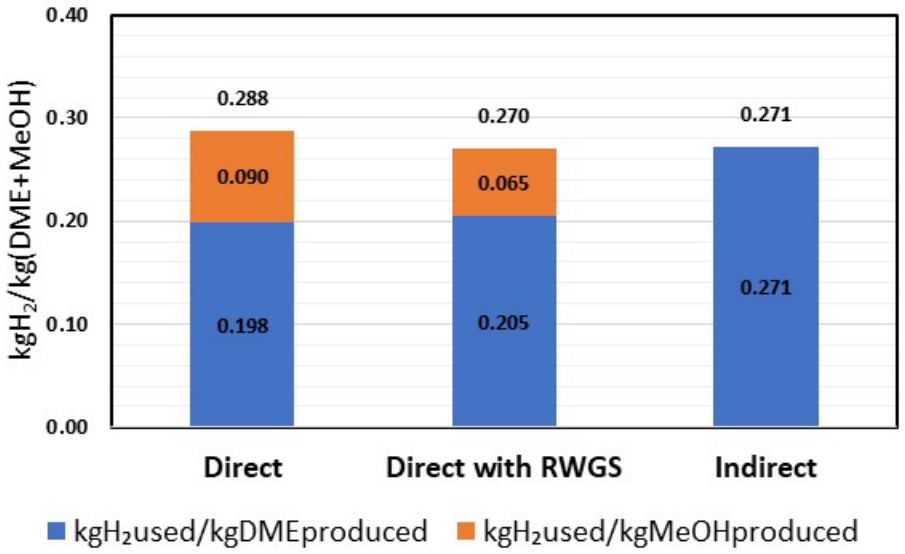

Figure 16. Hydrogen consumption of pathways

An observation should be made regarding the consumption of hydrogen in the production of DME and MeOH. There are notable differences between the product and byproduct fuels despite the relatively consistent total hydrogen quantity consumed. Specifically, within the Direct Method, a substantial 31% of hydrogen is used in the production of the byproduct. However, upon implementing the RWGS modification in the Direct Method, this percentage diminishes to 24%, indicating a more optimized allocation of hydrogen towards the desired product DME. On the other hand, in the Indirect Method, there is an efficient and complete utilization of hydrogen, signifying its complete allocation towards the intended product without deviation towards byproduct formation.

4.4. Process Energy Demand

The energy consumption results show that the Direct Method has a total energy usage of 573 MW. When the RWGS is integrated into the Direct Method, there is 2% rise in energy consumption, mainly due to the electrified RWGS reactor, resulting in a total energy demand of 586 MW. In contrast, the Indirect Method displays a significant 7% increase in energy demand from the baseline, resulting in a total energy consumption of 616 MW, as illustrated in Figure 17.

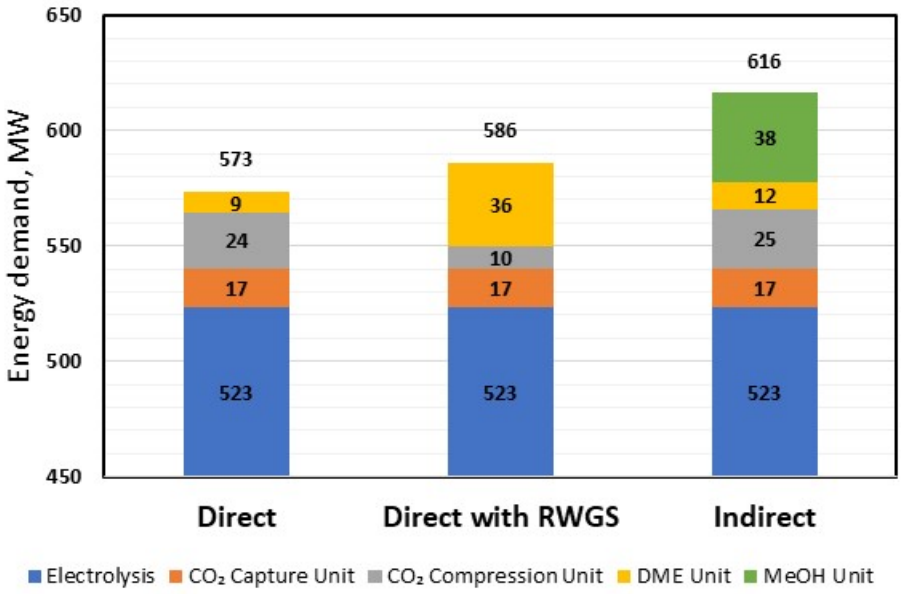

Figure 17. Overall energy demand of pathways

While the Direct Method may have lower energy demand compared to the other pathways, it does not make up for the better performance compared to the other approaches. The energy demands of each route increased due to design modifications, which will be delved into in further detail as follows.

It is notable to highlight that the most resource-intensive component across the three processes is hydrogen electrolysis, accounting for a substantial proportion ranging between 85 to 91% within each pathway. This uniformity in hydrogen source and carbon dioxide capture unit among the three methods results in equivalent consumption levels. However, distinct disparities emerge in the utilization of their remaining units, showcasing considerable differences among the pathways. Excluding the H_2 electrolysis, and CO_2 capture unit energy demands, in the Direct Method, a significant 73% of energy allocation is dedicated to the CO_2 compression unit, due to the necessary feed pressure of 70 bar required for processing in the DME unit. The remaining 27% of energy usage in the DME unit is split between compressors and refrigeration demand.

Subsequently, in the Direct Method modified with RWGS the energy demand of the CO_2 compression unit falls, due to the feed's necessity of being only at 5 bar to have the CO_2 transformed in the RWGS reactor, allocating only 21% of the energy demand. The DME unit on the other hand, has 65% of its usage due to the pressure changers, due to the need of the feed to be processed at 70 bar in the DME reactor, and the rest falls to the energy demand of the RWGS

reactor and refrigeration duty. Finally, in the Indirect Method, the CO_2 Compression Unit is responsible for 34% of the energy load as it is essential to have the CO_2 feed at 88 bar for processing in the MeOH Unit. The MeOH Unit, on the other hand, has a significant 50% energy demand, because of the electric heater that is used to supply the heat demand in the boiler. Meanwhile, the DME unit only accounts for 16% of the overall demand, mainly due to the energy requirement of the DME reactor.

4.5. Overall Efficiency

The energy value of each product was assessed by analyzing the Higher Heating Value (HHV) of both Dimethyl Ether (DME) and Methanol (MeOH) using Aspen Plus software. Hence, by calculating the total energy demand of the process in MW, we estimated the efficiency of each process using the equation (33).

$$HHV\ Efficiency = \frac{HHV\ of\ DME\ and\ MeOH\ products\ (MW)}{Total\ Energy\ Consumption\ (MW)} \quad (33)$$

The outcomes revealed an efficiency of 32.9% for the Direct Method, 35.1% for the Direct Method with RWGS modification, and finally, an efficiency of 35.6% for the Indirect Method, as can be seen in Figure 18.

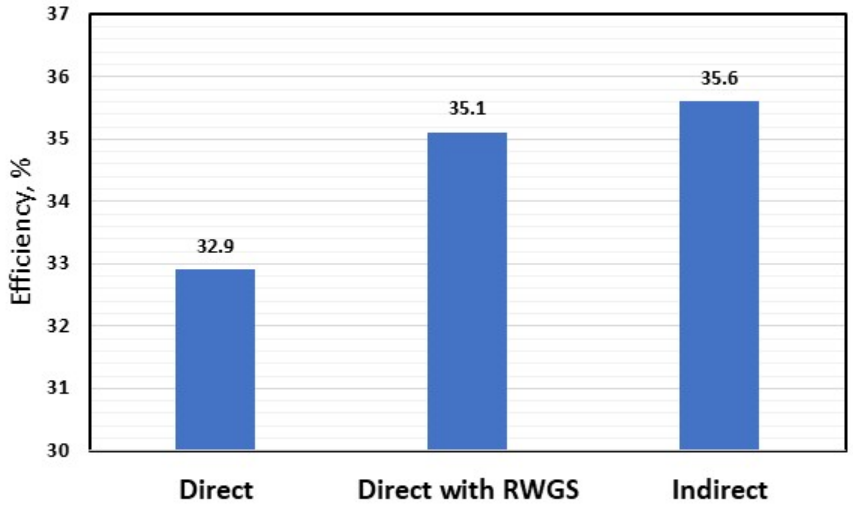

Figure 18. Efficiencies across pathways

The results align with the production rate of the pathways and their energy demand. Even though the Indirect Method has the highest energy consumption of the three, it is also the only pathway that doesn't produce a byproduct and has the highest production rate.

5. Techno-Economic Analysis

We compared the profitability estimations of three design pathways by using the Net Present Value (NPV), which is a financial measure that considers the income, expenses, investments, and other factors that affect the value of a project over time. The assessment was done over the year 2023, using as currency US dollars. The operation time is 7884 hours, considering the capacity factor of the plant to be 90%. Details of the TEA results are presented in the Appendix.

5.1. Assumptions

The feed and product prices, the reactor catalyst, and other cost parameters are adopted from different references and summarized in Table 16. The calculations of the capital investment costs for the different units were estimated with Aspen Process Economic Analyzer version 12 using the simulation files of the three pathways, we then calculated our total capital investment with the equation (34):

$$Total\ Capital\ Investment = Total\ Direct\ Costs + Total\ Indirect\ Costs + Working\ Capital + Startup \quad (34)$$

The operational cost estimation was calculated using the equation (35) [59]:

$$Operating\ Costs = RM + UC + OLC + MC + OHC + PIT + ECC + GE \quad (35)$$

Where:

RM: Raw material

UC: Utility Costs

OLC: Operating labor costs

MC: Maintenance costs

OHC: Overhead costs

PIT: Property insurance and taxes

ECC: Environmental control costs

GE: General expenses

Table 16. Economic evaluation assumptions

Feedstock and product prices	
Electricity charge, ¢/kWh	2.56 [60]
Electricity demand charge, $/kW	10.06 [60]
DME price, $/tonne	2050 [61]
MeOH price, $/tonne	430 [62]
Capital cost estimation	
PEM Electrolysis	1593 $/1kg$H_2$-day [41,63]
Direct DME catalyst	105.4 $/kg [64]
RWGS catalyst	119.3 $/kg [64]
MeOH catalyst	119.3 $/kg [64]
Indirect DME catalyst	11.6 $/kg [57]
Waste water disposal	0.44 $/tonne [64]
Cooling water	0.07 $/tonne [64]
Economic assumptions	
Operation time (h/year)	8760
Capacity factor (%)	90
Chemical engineering plant cost index	803.4 [65]
Plant lifetime (year)	30
Loan lifetime (year)	15
Interest rate on loan (%)	5
Debt percentage (%)	40
Inflation rate (%)	3
Federal + provincial tax rate (%)	26
Internal return rate (%)	10
Debt taken distribution	1st year: 8%, 2nd year: 60%, 3rd year: 32%

5.2. Capital Investment Costs

The capital cost estimation of all equipment is conducted by including their scale impact, the year of the previous estimation (the pricing basis of Aspen Process Economic Analyzer version 12 was the first quarter of 2019), and updating to 2023, as shown in equation (36). Where *n* is the scaling

factor, that can range from 0.5 to 1.0, and we are using the preliminary Chemical Engineering Plant Cost Index CEPCI for 2023 of 803.4 [65].

$$Cost = Reference\ Cost * \left(\frac{Capacity}{Reference\ Capacity}\right)^{n} * \left(\frac{CEPCI}{Reference\ CEPCI}\right) \quad (36)$$

Considering the total equipment cost, we proceeded to calculate the total direct cost and indirect costs to calculate the fixed capital investment and total capital investment with the parameters described in Table 17.

Table 17. Capital investment parameters used for CAPEX estimation [59]

CAPEX	**Value**
Delivery costs	8% of purchased equipment cost
Direct Costs (% of Equipment Delivered Costs)	
Installation cost	
Equipment erection	40%
Piping	70%
Instrumentation and Control	20%
Electrical	10%
Utility cost	10%
Off-sites	20%
Buildings	20%
Site preparation	10%
Land	6%
Indirect Costs (% of Equipment Delivered Costs)	
Engineering and supervision	22%
Construction overhead	18%
Project contingency	10% of fixed capital investment
Fixed Capital Investment (FCI) = Direct Costs + Indirect Costs	
Start-up costs	9% of fixed capital investment
Working Capital	15% of fixed capital investment
Total Capital Investment (TCI) = Fixed Capital Investment + Startup Costs +Working Capital	

Furthermore, we annualized the Total Capital Investment with an Interest Rate of 8% (Loan Interest plus Inflation Rate) and 30 years, using the equation (37).

$$Annualized\ capital\ cost = TCI * \frac{i(1+i)^n}{(1+i)^n - 1} \quad (37)$$

Where:

n: number of years

i: interest rate

5.3. Operating Costs

The cost of operation of the plant was calculated by assessing the keys variables such as the cost of raw materials, utilities, catalyst, labor, and materials for operating and maintaining it. Along with other fees, such as operational overhead and property insurance. For the labor cost, we took into consideration the labor wage rate of 21.81 ($/h) [66] as per the mean hourly wage in 2023, the type of process (continuous, fluid), the plant capacity (tonne/day), and applying the equation suggested in Perry's Chemical Engineers Handbook [67], the equation (38) was used:

$$\log Y = -0.783 * \log X + 1.252 \quad (38)$$

Where:

Y: labor operating hours per processing unit, h/tonne

X: plant capacity, tonne/day

Assuming 5 shifts, 40 hours of work per week, 52 working weeks per year, we calculated the Labor Wages ($/year):

$$LW\left(\frac{\$}{year}\right) = operators\ per\ shift * 5\ shifts * 2080\ hours\ per\ year * labour\ wage\ rate \quad (39)$$

The considerations for maintenance overhead, business services, environmental control costs and administrative expenses are summarized in Table 18.

Table 18. Operating cost parameters used for OPEX estimation [59]

OPEX	**Value**
Operating Labor Costs	
Labor Wages, $/h	21.81 [67]
Supervision and engineering	22% of Labor Wages
Operating supplies and services	6% of Labor Wages
Laboratory expenses	15% of Labor Wages
Payroll charges	35% of Labor Wages + Supervision and Engineering costs
Maintenance Costs	
Maintenance wages	3.5% of Fixed Capital Investment (excluding land)
Maintenance supervision and engineering	25.0% of the Maintenance Wages
Material supplies	100.0% of the Maintenance Wages
Maintenance overhead	5.0% of the Maintenance Wages
Overhead Costs	
Plant overhead	7.1% of the TWSE
Mechanical department services	2.4% of the TWSE
Employee relations department	5.9% of the TWSE
Business services	7.4% of the TWSE
Property insurance and taxes, $/year	2.0% of Fixed Capital Investment
General Expenses	
Sale expenses	3.0% of Sales
Research and development	5.0% of Sales
Administrative expenses	3.0% of Sales

*TWSE is the total operating and maintenance wages, supervision, and engineering expenses

5.4. Economic Evaluation

With all the considerations explained above, here we can see a detailed analysis of each process. The cost analysis results show that the direct capital cost of the Direct Method with RWGS is 7% higher compared to the Direct Method due to the additional equipment that RWGS requires. The Indirect Method is 11% more expensive, due to the MeOH Unit.

Moreover, the total capital cost and operating cost of the Direct Method are much lower than the other two pathways by approximately 9%. However, its minimum selling price is 61% above the

market price. This is attributed to the incomplete conversion of CO_2 to DME, which makes the baseline method have a total revenue of 401.0 $Million, and a MSP of 3287 $/tonne. The Direct Method with RWGS provides an improvement in the process, due to a better conversion of CO to DME. It offers a MSP of 3049 $/tonne, but it's still 49% above market price, for a Total Revenue of 431.7 $Million. It can be seen that the Indirect Method is the best pathway with the lowest MSP, it offers a Total Revenue of 437.9 $Million, and a MSP of 2465 $/tonne, which is only 20% above the market price.

Table 19. Economic analysis summary of three pathways

Direct capital cost, $Million	**Direct**	**Direct with RWGS**	**Indirect**
PEM Electrolyzer	259.8	259.8	259.8
CO_2 Capture + Compression	212.1	212.1	212.1
DME and MeOH synthesis & recovery (Direct or Direct with RWGS)	19.9	54.1	-
MeOH production and recovery (Indirect)	-	-	71.1
DME production and recovery (Indirect)	-	-	1.8
Steam Boiler	1.6	1.0	4.1
CAPEX and OPEX, $Million/year			
Total capital cost (equipment, direct, indirect)	96.5	106.5	107.5
Total operating cost (operating labor, maintenance, overhead, environmental control, general)	303.5	324.8	330.0
Sale at 90% of design capacity			
Minimum Selling Prince DME, $/tonne	3287	3049	2465
Total revenue at MSP, $Million/year	401.0	431.7	437.9

5.5. Sensitivity Analysis

One of the key uncertainties is the impact of the electricity price on the profitability of each pathway. Figure 19 illustrates how DME's Minimum Selling Price (MSP) changes with different electricity prices for all three routes: Direct, Direct with RWGS and Indirect.

Three provinces in Canada, which have access to a power grid with 70% to 99% supplied by renewable resources, are selected for analysis [68]: 1) Quebec, which has an electricity rate of 0.026 ($/kWh) and a monthly billing demand of 10.06 ($/kW) [60], 2) British Columbia with 0.045 ($/kWh) and 9.13 ($/kW), respectively, and a basic charge of 0.020 ($/day) [69], and lastly, 3) New Brunswick with, an electricity rate of 0.043 ($/kWh) and billing demand 11.64 ($/kW) [70]. The purpose of analyzing different provinces is to assess the feasibility of three pathways in various energy scenarios. While British Columbia and Quebec generate electricity from non-emitting sources, New Brunswick has mixed sources. Approximately one-third of its energy comes from fossil fuels [68].

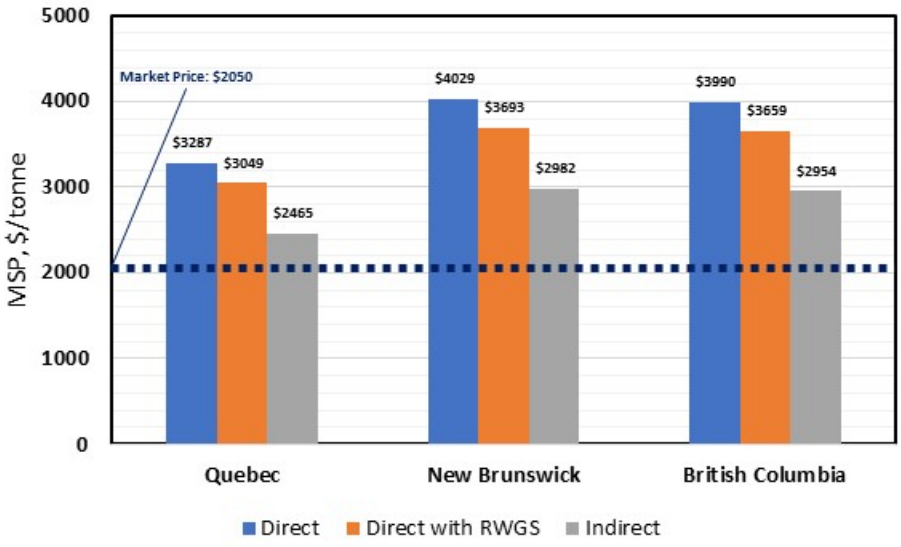

Figure 19. Effect of electricity price of provinces on Minimum Selling Price of DME

To have a better understanding of the changes in the electricity rate, a sensitivity analysis with a constant billing demand (same as that of Quebec) is conducted and results are shown in Figure 20.

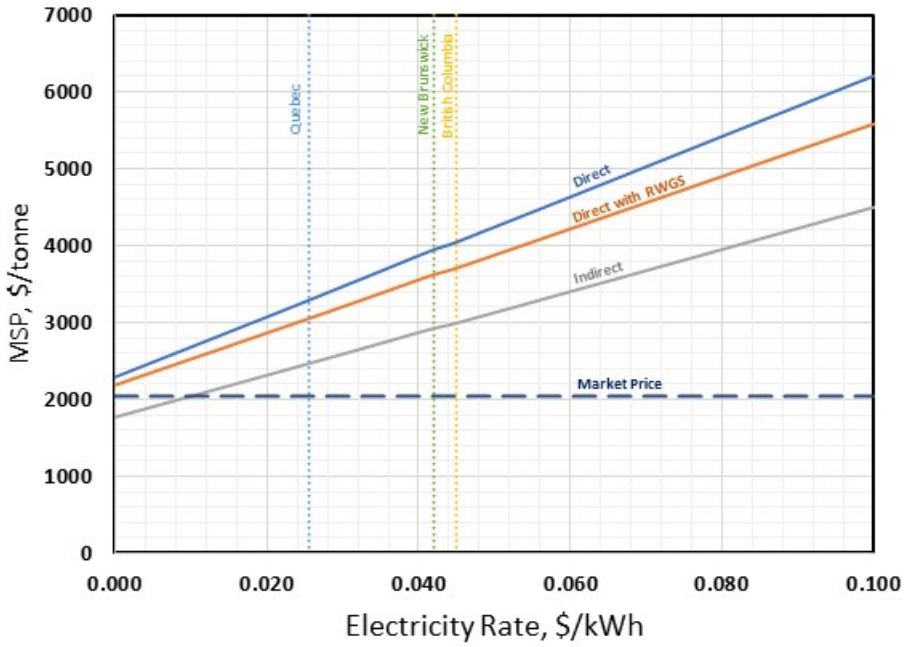

Figure 20. Effect of Electricity Rate on the Minimum Selling Price of DME

It can be observed that all processes are equally sensitive to the change in price. Quebec is the best option to provide electricity, which achieves the minimum selling price of 2465 ($/tonne) with the Indirect Method.

In terms of comparing our three pathways the Direct Method is the least competitive among the three, even with the lowest energy consumption, the production rate is lower than the rest. The Direct Method modified with RWGS shares a similar energy consumption than the base model, with a slight improvement of 18% in the production rate of DME. Finally, even with the highest energy consumption, the Indirect Method produces 54% more DME compared to the Direct method, which makes it the best approach for the DME production from CO_2.

6. GHG Analysis

The lifecycle greenhouse gas emission analysis of the three pathways for DME production and their electricity source were done using a midpoint impact evaluation with the TRACI 2.1 impact assessment method in the OpenLCA version 1.11 software. Within the scope, it was considered all of the units and its electricity, as can be appreciated in Figure 21. The functional unit of this analysis is kg CO_2 eq/kg DME.

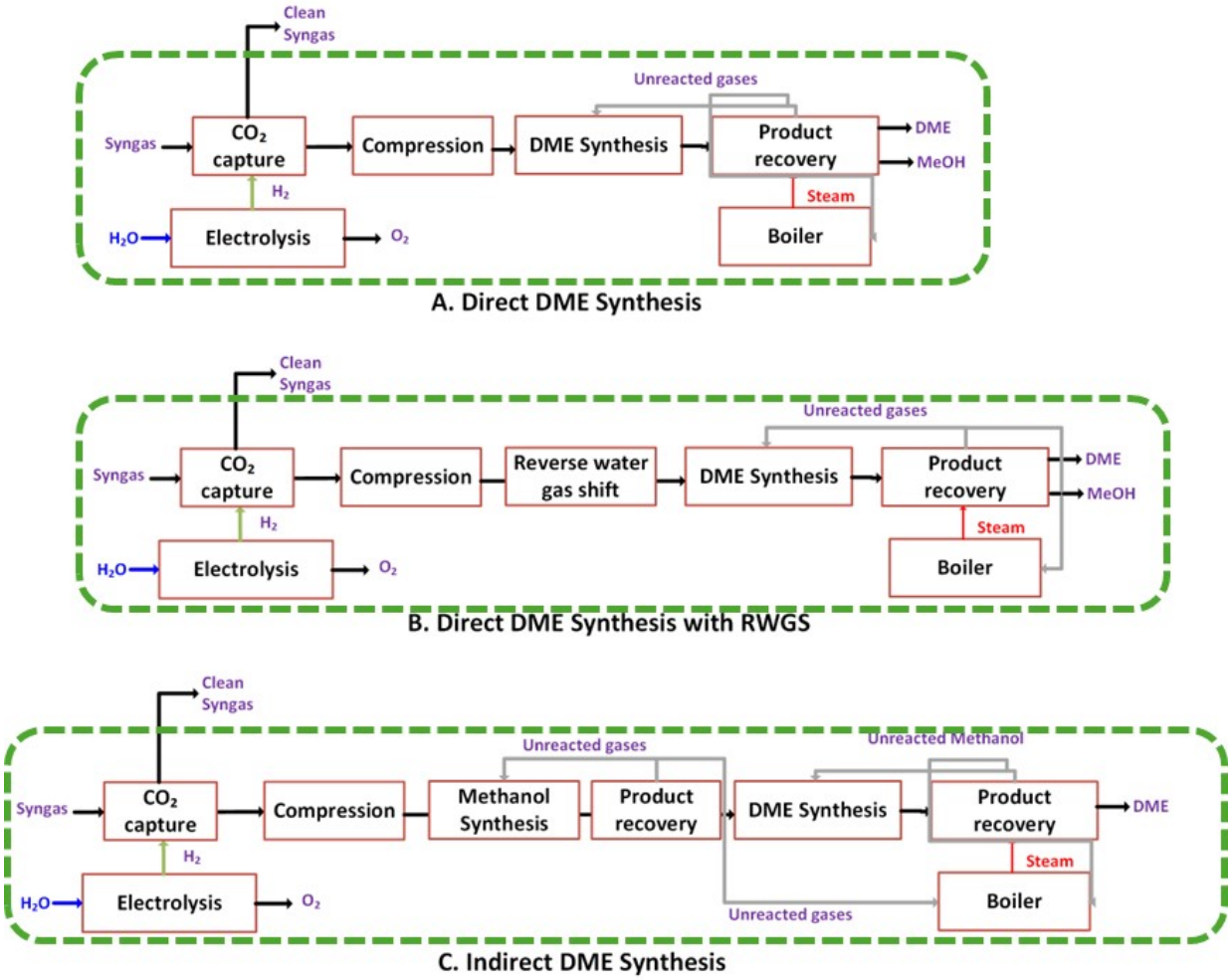

Figure 21. Scope of the LCA of the pathways

We evaluated three provinces: Quebec, British Columbia and New Brunswick. The reference processes for the ecoinvent database version 3.8 used in this assessment are described in Table 20.

Table 20. Reference processes from Ecoinvent database

Product Name	Reference Process	Location	Process UUID
electricity, high voltage	electricity, high voltage, production mix | electricity, high voltage | APOS, S	Canada, Quebec	b0f863e6-5542-3b70-a932-cf18903aa825
	electricity, high voltage, production mix | electricity, high voltage | APOS, S	Canada, British Columbia	808d59d3-18c5-3974-bc9a-151f3ee67cb2
	electricity, high voltage, production mix | electricity, high voltage | APOS, S	Canada, New Brunswick	cdfdab6c-bc39-3ac2-847e-3c4bdc2c7325
methanol production	methanol production | methanol | APOS, S	Global	07af5466-c58d-31d4-8e4c-187718df1a38
dimethyl ether production	dimethyl ether production | dimethyl ether | APOS, S	Rest-of-World	368ecdbb-f029-3fd3-ae45-434e001fe7c6

The results are summarized in Figure 21. The referenced production of DME represents 1 kg in gaseous state, it comes from production of methanol (from natural gas) with a process yield of 95%, the data used has no specific geographical origin, average European data are used for raw materials, transport requirements and electricity mix [71]. We considered two scenarios, the first one doesn't include the GHG emissions of the MeOH production, in the second one, we took it into consideration, since it's a more comprehensive approach.

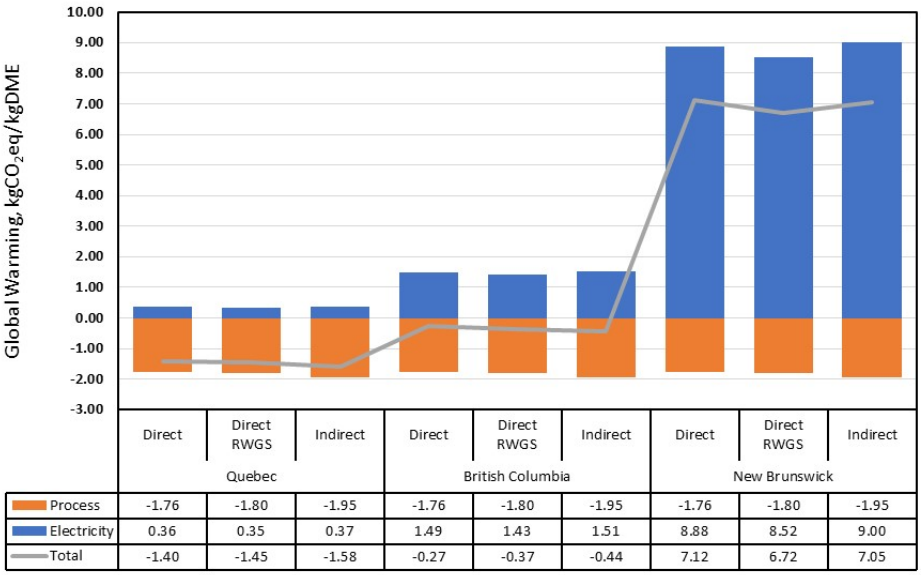

	Quebec			British Columbia			New Brunswick		
	Direct	Direct RWGS	Indirect	Direct	Direct RWGS	Indirect	Direct	Direct RWGS	Indirect
Process	-1.76	-1.80	-1.95	-1.76	-1.80	-1.95	-1.76	-1.80	-1.95
Electricity	0.36	0.35	0.37	1.49	1.43	1.51	8.88	8.52	9.00
Total	-1.40	-1.45	-1.58	-0.27	-0.37	-0.44	7.12	6.72	7.05

A. Without GHG emissions of MeOH production

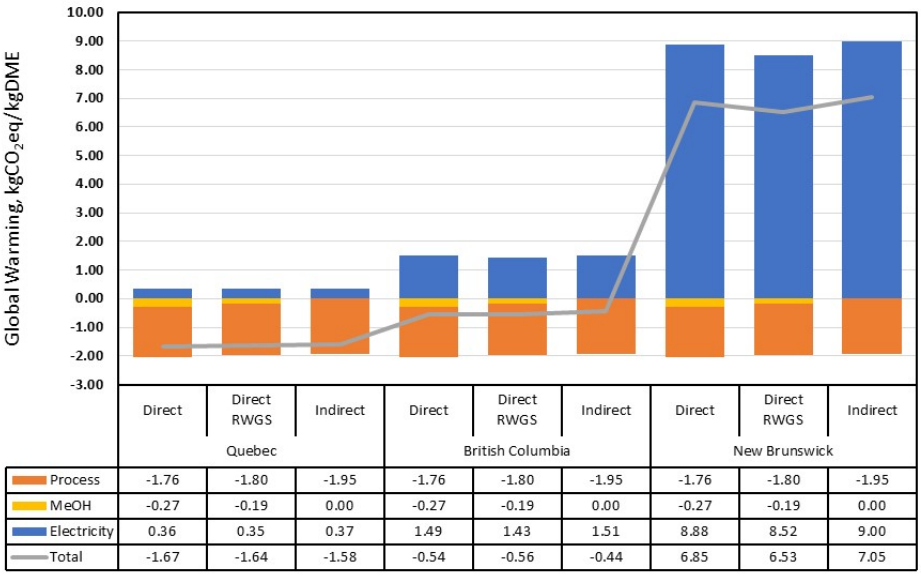

	Quebec			British Columbia			New Brunswick		
	Direct	Direct RWGS	Indirect	Direct	Direct RWGS	Indirect	Direct	Direct RWGS	Indirect
Process	-1.76	-1.80	-1.95	-1.76	-1.80	-1.95	-1.76	-1.80	-1.95
MeOH	-0.27	-0.19	0.00	-0.27	-0.19	0.00	-0.27	-0.19	0.00
Electricity	0.36	0.35	0.37	1.49	1.43	1.51	8.88	8.52	9.00
Total	-1.67	-1.64	-1.58	-0.54	-0.56	-0.44	6.85	6.53	7.05

B. With GHG emissions of MeOH production

Figure 22. GHG impact contribution by province, (a) without avoided emissions of MeOH, and (b) with avoided emissions of MeOH

Quebec and British Columbia are both provinces with low greenhouse intensity for their electricity production, having 14.92 g and 61.34 g of CO_2e/kWh respectively in 2019. The LCA results show that the global warming impact in Quebec is consistently lower in all three pathways. In the province of New Brunswick, there is an impact of 365.67 g of CO_2e/kWh, making it a province where all CCU-DME pathways would have positive GHG emissions.

Having established Quebec as the best option for a province for viability, then we proceed to analyze the behavior of the three pathways with the avoided emissions from MeOH production and their demand for GHG credits. The GHG avoided credits were also calculated with Carbon intensities from 0 to 100 tonCO_2/MWh, using the formula (40), and as reference the production of DME from natural gas, that has a GHG emission of 1310.70 g of CO_2eq/kgDME and a DME market price of 2.05 $/kg:

$$Avoided\ GHG\ Credit = \left\{\frac{MSP_{3PW} - MAP}{GHG_{NG} - GHG_{3PW}}\right\} \quad (40)$$

Where:

MSP_{3PW}: DME min. selling price of 3PathWays-DME process ($/kg DME)

MAP: Market Price of DME ($/kg DME)

GHG_{3PW}: GHG emissions from 3PathWays-DME process (kg CO_2 eq/kg DME)

$GHG_{NG\text{-}DME}$: GHG emissions from NG-DME process (kg CO_2 eq/kg DME)

Figure 22 illustrates the changes in the cost of avoided/captured emissions as a function of carbon intensity. The three pathways exhibit comparable sensitivity to variations in carbon intensity. The Direct Method with RWGS demonstrates a slightly lower credit demand for the avoided emissions in contrast to the Indirect Method employing, and notably lower compared to the standard Direct Method.

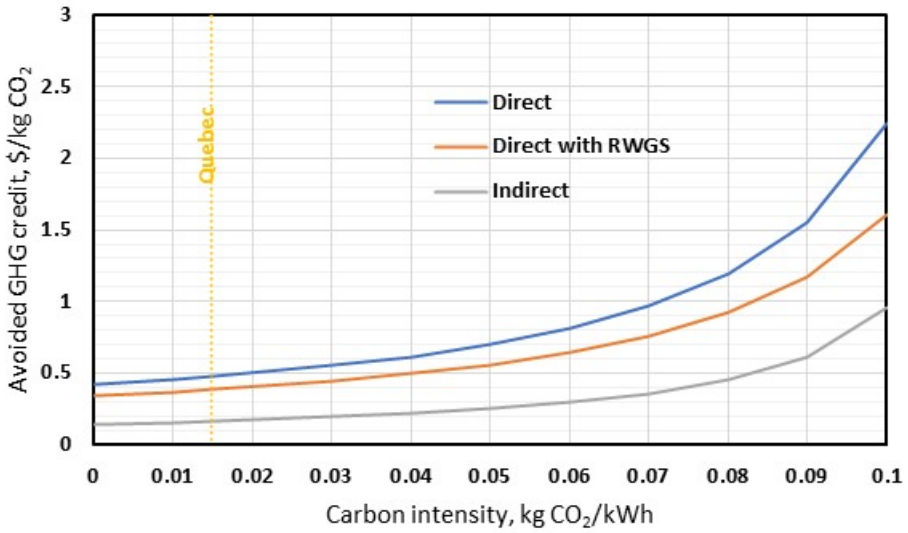

Figure 23. Avoided GHG credit required of pathways required for different carbon intensity

Despite the absence of emissions from the electric grid, and because the Direct Method has the highest MSP, at 0 $kgCO_2/MWh$ of carbon intensity, it requires an avoided GHG emission of 0.415 $\$/kgCO_2$, while the Direct Method with RWGS requires 0.339 $\$/kgCO_2$, which represents a 18% decrease, the Indirect Method needs a support of 0.143 $\$/kgCO_2$, which is 65% lower than the Direct Method. Once there is presence of GHG emissions at 0.01492 $kgCO_2/kWh$ of carbon intensity, resembling the carbon intensity of the Quebec, the Direct Method needs an avoided GHG credit of 0.472 $\$/kgCO_2$, while the Direct Method with RWGS needs 0.384 $\$/kgCO_2$, and the Indirect Method requires 0.164 $\$/kgCO_2$, this trend is in accordance with the delta of the market price and the minimum selling price, which is constant, and the delta of GHG emissions, that change based on the ratio of energy consumption per mass of fuel produced. To elaborate further, the Direct Method requires 24.3 kWh per kilogram (DME+MeOH), the Direct Method with RWGS demands 23.3 kWh per kilogram (DME+MeOH), and the Indirect Method necessitates 24.6 kWh per kilogram (DME+MeOH). This difference in the pathways is consistent with a carbon intensity of 0.1 $kgCO_2/kWh$, the three pathways have avoided GHG emissions of 2.242 $\$/kgCO_2$ for the Direct Method, 1.609 $\$/kgCO_2$ for the Direct Method with RWGS, and 0.958 $\$/kgCO_2$ for the Indirect, where the Direct Method with RWGS shows a decrease of 28% compared to the Direct Method, likewise, the Indirect Method shows a decrease by 57% compared to the Direct Method, this is because it shows the smaller delta in the market price and the minimum selling price of DME, which has a bigger impact than the smaller delta of GHG emissions between the three pathways and the DME produced from natural gas. Overall, this indicates, that from the three pathways, the Indirect Method is the most favorable, given its closeness of the minimum selling price and the market price, which is only 20% above.

7. Conclusion

The main goal of this research was to design and evaluate three different methods for producing dimethyl ether from carbon dioxide. The aim is to establish a more environmentally friendly and economically beneficial alternative to current industry practices. After conducting comprehensive simulations, techno-economic analyses, and environmental impact assessments, the generated production rates and data for efficiency evaluations suggest the Indirect Method was found to be the most viable pathway, among the alternatives considered.

In regard to the singular production rate of dimethyl ether (DME), the focal product of interest, the Direct Method exhibits a lower performance when compared with alternative methods. In contrast, the Direct Method yields 16229 kg/h of DME, whereas the Direct Method incorporating the RWGS process generates 19103 kg/h, and notably, the Indirect Method achieves a higher production rate of 25040 kg/h. Consequently, the Indirect Method proves to be the most effective, showcasing a 54% increase in production compared to the Direct Method and a 31% enhancement over the Direct Method with RWGS.

In terms of overall efficiency, comparable results are observed across the evaluated pathways. The Direct Method demonstrates an efficiency of 32.9%, while the integration of RWGS enhances the efficiency to 35.1%. Notably, the Indirect Method exhibits the highest efficiency at 35.6%. This outcome arises from the distinct characteristics of each method: despite the lower energy demand exhibited by both the Direct Method and its RWGS-modified counterpart, the concurrent production of methanol as a byproduct reduces the higher heating value (HHV) of the resulting products. Despite its comparatively higher energy demand, the Indirect Method exclusively produces dimethyl ether (DME) as its sole product, thus rendering it the most efficient pathway among the evaluated options.

From an economic standpoint, an analysis was conducted on the minimum selling price of dimethyl ether and the total revenue generated by each pathway. The Direct Method attains an MSP of 3287 $/tonne, yielding a total revenue of 401.0 $Million/year. Comparatively, the Direct Method incorporating RWGS exhibits an MSP of 3049 $/tonne and generates a total revenue of 431.7 $Million/year. In contrast, the Indirect Method achieves an MSP of 2465 $/tonne, signifying

a 25% decrease concerning the Direct baseline and 19% the decrease regarding the Direct modified with RWGS, while simultaneously achieving a total revenue of 437.9 $Million/year, indicating a 9% and 1% increase in comparison to the Direct baseline and modified figures respectively. The economic evaluation demonstrated that the Indirect Method, despite having an MSP that exceeds the prevailing market price of DME by 20%, emerges as the most advantageous approach.

In terms of the environmental impacts attributed to greenhouse gas (GHG) emissions, the Direct Method demonstrates inferior performance relative to the other pathways. This is discernible in the different carbon intensity scenarios, where this method even with lowest emissions compared to the remaining two pathways, it still holds the biggest delta of the market price a minimum selling price. Such discrepancies manifest in higher Avoided GHG credits, as exemplified in the province of Quebec. The Direct Method with RWGS displays an enhanced performance relative to the Direct Method. Nevertheless, it continues to require higher avoided credit compared to the Direct Method. The Indirect pathway notably presents the most competitive outcome by having the most viable minimum selling price, thereby resulting in the lowest GHG avoided credit among the evaluated pathways.

In conclusion, according to our results, TEA and LCA, it can be concluded that the Indirect Method is the most efficient pathway. Its production rate, CO_2 utilization, H_2 consumption, overall efficiency, indicate that the Indirect Method is the optimal pathway among the three, displaying superior performance, energy efficiency, and economic viability. However, there is still room for greater process improvement and optimization in terms of energy usage, which might lead to overall enhancements across all analyzed elements.

7.1. Future Works

The next phase of this research will focus on increasing the efficiency of the Indirect Method, with a particular emphasis on decreasing the energy requirements in hydrogen production, which now accounts for 85% of overall demand. The integration of alternative technology is expected to significantly improve all aspects of the process.

8. Appendix

8.1. Capital Expenditures

Pathway	Direct	Direct with RWGS	Indirect
Total equipment cost (TEC)			
Equipment Cost	$216,431,355	$248,213,492	$242,301,170
Delivery Cost	$17,314,508	$19,857,079	$19,384,094
Equipment Delivered Cost	**$233,745,863**	**$268,070,571**	**$261,685,264**
Installation cost (INST)	**$17,161,325**	**$19,009,004**	**$46,908,996**
Catalysts	**$4,322,062**	**$10,357,140**	**$3,396,588**
Total equipment cost	**$255,229,250**	**$297,436,715**	**$311,990,848**
Total direct cost (TDC)			
TEC	*$255,229,250*	*$297,436,715*	*$311,990,848*
Utility cost	*$23,374,586*	*$26,807,057*	*$26,168,526*
Off-sites	*$46,749,173*	*$53,614,114*	*$52,337,053*
Buildings	*$46,749,173*	*$53,614,114*	*$52,337,053*
Site preparation	*$23,374,586*	*$26,807,057*	*$26,168,526*
Land	*$14,024,752*	*$16,084,234*	*$15,701,116*
Total direct cost	**$409,501,520**	**$474,363,292**	**$484,703,122**
Total indirect cost (TIC)			
Engineering and supervision	*$51,424,090*	*$58,975,526*	*$57,570,758*
Construction overhead	*$42,074,255*	*$48,252,703*	*$47,103,347*
Project contingency	*$55,888,874*	*$64,621,280*	*$65,486,359*
Total direct cost	**$149,387,219**	**$171,849,508**	**$170,160,464**
Fixed Capital Investment (FCI)	**$558,888,739**	**$646,212,800**	**$654,863,587**
Working Capital	$107,503,893	$124,300,933	$125,964,937
Start-up costs	$50,299,987	$58,159,152	$58,937,723
Total Capital Investment (TCI)	**$1,086,687,313**	**$1,198,667,579**	**$1,209,760,941**
Annulized CAPEX			
Interest rate	8.0%	8.0%	8.0%
Annulalization factor	8.9%	8.9%	8.9%
Annualized capital cost, $/yr	**$96,527,645**	**$106,474,565**	**$107,459,959**
$Million/yr	***$96.5***	***$106.5***	***$107.5***

8.2. Operational Expenditures

Pathway	Direct	Direct with RWGS	Indirect
Total revenue, $/yr	$400,999,493	$431,726,041	$437,927,723
$Million/yr	$401.0	$431.7	$437.9
Raw Material, $/yr	$3,595,066	$8,494,381	$3,732,845
Utilities, $/yr	$158,618,728.8	$162,206,807.7	$170,505,958.9
Operating labour costs (OLC)			
Calculation method	Seider	Seider	Seider
Seider method			
Number of operators per shift	9	9	9
Operation impact	9	9	9
Scale impact	18	18	18
Perry's handbook			
labour hours per processing unit, h/ton	0.197371687	0.173716715	0.140546903
Number of operators per shift	29	30	32
Total number of operators per shift	18	18	18
Number of shifts	5	5	5
Labour wages, $/yr	$4,082,832	$4,082,832	$4,082,832
Supervision and engineering, $/yr	$898,223	$898,223	$898,223
Operating supplies and services, $/yr	$244,970	$244,970	$244,970
Laboratory expenses, $/yr	$612,425	$612,425	$612,425
Payroll charges, $/yr	$1,743,369	$1,743,369	$1,743,369
Operating labour costs, $/yr	**$7,581,819**	**$7,581,819**	**$7,581,819**
Maintenance costs (MC)			
Maintenance wages, $/yr	$19,070,240	$22,054,500	$22,370,686
Maintenance supervision and engineering, $/yr	$4,767,560	$5,513,625	$5,592,672
Material supplies, $/yr	$19,070,240	$22,054,500	$22,370,686
Maintenance overhead, $/yr	$953,512	$1,102,725	$1,118,534
Maintenance costs, $/yr	**$43,861,551**	**$50,725,350**	**$51,452,579**
Overhead costs (OHC)			
Plant overhead, $/yr	$2,046,139	$2,310,992	$2,339,053
Mechanical department services, $/yr	$691,653	$781,180	$790,666
Employee relations department, $/yr	$1,700,312	$1,920,402	$1,943,720
Business services, $/yr	$2,132,595	$2,408,639	$2,437,887
Overhead costs, $/yr	**$6,570,699**	**$7,421,213**	**$7,511,326**
Property insurance and taxes, $/yr	**$11,177,775**	**$12,924,256**	**$13,097,272**
General expenses (GE)			
Sale expenses, $/yr	$12,029,984.78	$12,951,781.22	$13,137,831.68
Research and development, $/yr	$20,049,974.63	$21,586,302.04	$21,896,386.13
Administrative expenses, $/yr	$12,029,984.78	$12,951,781.22	$13,137,831.68
General expenses, $/yr	**$44,109,944**	**$47,489,864**	**$48,172,049**
Operating costs, $/yr	**$303,465,270**	**$324,793,379**	**$330,003,537**
$Million/yr	***$303.5***	***$324.8***	***$330.0***

8.3. Net Present Value

Pathway	Direct	Direct with RWGS	Indirect
Gross Earning, $/yr	$97,534,222	$106,932,662	$107,924,185
Debt needed, $	$434,674,925	$479,467,032	$483,904,376
Equity Expended, $	$652,012,388	$719,200,548	$725,856,565
Debt Taken, (End of 1st yr)	$36,512,694	$40,275,231	$40,647,968
Debt Taken, (End of 2nd yr)	$312,183,531	$344,353,222	$347,540,123
Debt Taken, (End of 3rd yr)	$473,843,483	$522,671,806	$527,509,000
Annual loan payment, $	$45,651,165	$50,355,397	$50,821,424
Return on Investment (ROI)	6.6%	6.6%	6.6%
Venture Profit	-$14,759,661	-$16,763,237	-$16,916,978
Land Value, $Million	$14	$16	$16
NPV, $Million	**$0**	**$0**	**$0**

9. Bibliography

[1] Bayu Prabowo, Mi Yan, Mochamad Syamsiro, Roy Hendroko Setyobudi, Muhammad Kunta Biddinika. State of the Art of Global Dimethyl Ether Production and It's Potentional Application in Indonesia. Proceedings of the Pakistan Academy of Sciences 2017;54 (1):29–39.

[2] Alternative Fuels Data Center: Dimethyl Ether n.d. https://afdc.energy.gov/fuels/emerging_dme.html (accessed March 21, 2024).

[3] Semelsberger TA, Borup RL, Greene HL. Dimethyl ether (DME) as an alternative fuel. Journal of Power Sources 2006;156:497–511. https://doi.org/10.1016/j.jpowsour.2005.05.082.

[4] Lee U, Han J, Wang M, Ward J, Hicks E, Goodwin D, et al. Well-to-Wheels Emissions of Greenhouse Gases and Air Pollutants of Dimethyl Ether from Natural Gas and Renewable Feedstocks in Comparison with Petroleum Gasoline and Diesel in the United States and Europe. SAE Int J Fuels Lubr 2016;9:546–57. https://doi.org/10.4271/2016-01-2209.

[5] Alba Carrero Parreño, Juan Diego Medrano García, Natalia Quirante. Carbon CO2 Reuse in Direct DME Synthesis from Syngas 2017.

[6] Machida H, Esaki T, Yamaguchi T, Norinaga K. Energy-Saving CO_2 Capture by H_2 Gas Stripping for Integrating CO_2 Separation and Conversion Processes. ACS Sustainable Chem Eng 2020;8:8732–40. https://doi.org/10.1021/acssuschemeng.0c02459.

[7] Kawai E, Ozawa A, Leibowicz BD. Role of carbon capture and utilization (CCU) for decarbonization of industrial sector: A case study of Japan. Applied Energy 2022;328:120183. https://doi.org/10.1016/j.apenergy.2022.120183.

[8] Grant Hauber. Norway's Sleipner and Snøhvit CCS: Industry models or cautionary tales? 2023.

[9] Peter Styring, Daan Jansen. Carbon Capture and Utilisation in the green economy 2012.

[10] Cuéllar-Franca RM, Azapagic A. Carbon capture, storage and utilisation technologies: A critical analysis and comparison of their life cycle environmental impacts. Journal of CO2 Utilization 2015;9:82–102. https://doi.org/10.1016/j.jcou.2014.12.001.

[11] United Nations Framework Convention on Climate Change. Paris Agreement 2016.

[12] United Nations Industrial Development Organization, Organisation for Economic Development & International Energy Agency. Technology Roadmap: Carbon Capture and Storage in Industrial Applications 2011.

[13] Singh B, Strømman AH, Hertwich EG. Comparative life cycle environmental assessment of CCS technologies. International Journal of Greenhouse Gas Control 2011;5:911–21. https://doi.org/10.1016/j.ijggc.2011.03.012.

[14] Farla JCM, Hendriks CA, Blok K. Carbon dioxide recovery from industrial processes. Climatic Change 1995;29:439–61. https://doi.org/10.1007/BF01092428.

[15] Salkuyeh YK, Mofarahi M. Reduction of CO_2 capture plant energy requirement by selecting a suitable solvent and analyzing the operating parameters: CO_2 capture, chemical solvent, power plant, energy, absorption. Int J Energy Res 2013;37:973–81. https://doi.org/10.1002/er.2899.

[16] George Olah - Industrial Scale Renewable Methanol Plant. CRI - Carbon Recycling International n.d. https://carbonrecycling.com/projects/george-olah (accessed March 30, 2024).

[17] Yang N, Kang F, Liu Z, Ge X, Zhou Y. An integrated CCU-plant scheme and assessment for conversion of captured CO2 into methanol. International Journal of Low-Carbon Technologies 2022;17:550–62. https://doi.org/10.1093/ijlct/ctac038.

[18] Chauvy R, Dubois L, Thomas D, De Weireld G. Techno-Economic and Environmental Assessment of Carbon Capture at a Cement Plant and CO2 Utilization in Production of Synthetic Natural Gas. SSRN Journal 2021. https://doi.org/10.2139/ssrn.3811432.

[19] Michailos S, Sanderson P, Villa Zaragoza A, McCord S, Armstrong K, Styring P, et al. Methanol Worked Examples for the TEA and LCA Guidelines for CO2 Utilization. Global CO2 Initiative 2018. https://doi.org/10.3998/2027.42/145723.

[20] Azizi Z, Rezaeimanesh M, Tohidian T, Rahimpour MR. Dimethyl ether: A review of technologies and production challenges. Chemical Engineering and Processing: Process Intensification 2014;82:150–72. https://doi.org/10.1016/j.cep.2014.06.007.

[21] Wang Y, Wang W, Chen Y, Zheng J, Li R. Synthesis of dimethyl ether from syngas using a hierarchically porous composite zeolite as the methanol dehydration catalyst. Journal of Fuel Chemistry and Technology 2013;41:873–80. https://doi.org/10.1016/S1872-5813(13)60037-7.

[22] Shukurov J, Fayzullaev N. Direct synthesis of dimethyl ether from synthesis gas, Namangan, Uzbekistan: 2024, p. 060042. https://doi.org/10.1063/5.0197641.

[23] Vakili R, Eslamloueyan R. Design and Optimization of a Fixed Bed Reactor for Direct Dimethyl Ether Production from Syngas Using Differential Evolution Algorithm. International Journal of Chemical Reactor Engineering 2013;11:147–58. https://doi.org/10.1515/ijcre-2012-0026.

[24] Poto S, Vink T, Oliver P, Gallucci F, Neira d′Angelo MF. Techno-economic assessment of the one-step CO2 conversion to dimethyl ether in a membrane-assisted process. Journal of CO2 Utilization 2023;69:102419. https://doi.org/10.1016/j.jcou.2023.102419.

[25] Kiss A.A., Suszwalak D.J.P.C., Ignat R. Process intensification alternatives in the dme production. Chemical Engineering Transactions 2013;35:91–6. https://doi.org/10.3303/CET1335015.

[26] Farsi M, Jahanmiri A, Eslamloueyan R. Modeling and Optimization of MeOH to DME in Isothermal Fixed-bed Reactor. International Journal of Chemical Reactor Engineering 2010;8. https://doi.org/10.2202/1542-6580.2063.

[27] Tavan Y, Hosseini SH, Ghavipour M, Khosravi Nikou MR, Shariati A. From laboratory experiments to simulation studies of methanol dehydration to produce dimethyl ether—Part I: Reaction kinetic study. Chemical Engineering and Processing: Process Intensification 2013;73:144–50. https://doi.org/10.1016/j.cep.2013.06.006.

[28] Peinado C, Liuzzi D, Sluijter SN, Skorikova G, Boon J, Guffanti S, et al. Review and perspective: Next generation DME synthesis technologies for the energy transition. Chemical Engineering Journal 2024;479:147494. https://doi.org/10.1016/j.cej.2023.147494.

[29] Nakyai T, Patcharavorachot Y, Arpornwichanop A, Saebea D. Comparative exergoeconomic analysis of indirect and direct bio-dimethyl ether syntheses based on air-steam biomass gasification with CO2 utilization. Energy 2020;209:118332. https://doi.org/10.1016/j.energy.2020.118332.

[30] Wu T-W, Chien I-L. A novel energy-efficient process of converting CO2 to dimethyl ether with techno-economic and environmental evaluation. Chemical Engineering Research and Design 2022;177:1–12. https://doi.org/10.1016/j.cherd.2021.10.013.

[31] González-Castaño M, Dorneanu B, Arellano-García H. The reverse water gas shift reaction: a process systems engineering perspective. React Chem Eng 2021;6:954–76. https://doi.org/10.1039/D0RE00478B.

[32] Zhuang Y, Currie R, McAuley KB, Simakov DSA. Highly-selective CO2 conversion via reverse water gas shift reaction over the 0.5wt% Ru-promoted Cu/ZnO/Al2O3 catalyst. Applied Catalysis A: General 2019;575:74–86. https://doi.org/10.1016/j.apcata.2019.02.016.

[33] Dzuryk S, Rezaei E. Intensification of the Reverse Water Gas Shift Reaction by Water-Permeable Packed-Bed Membrane Reactors. Ind Eng Chem Res 2020;59:18907–20. https://doi.org/10.1021/acs.iecr.0c02213.

[34] Reina TR, Odriozola JA, Arellano-Garcia H, editors. Engineering solutions for CO2 conversion. Weinheim: Wiley-VCH; 2021.

[35] Shekari A, Labrecque R, Larocque G, Vienneau M, Simoneau M, Schulz R. Conversion of CO2 by reverse water gas shift (RWGS) reaction using a hydrogen oxyflame. Fuel 2023;344:127947. https://doi.org/10.1016/j.fuel.2023.127947.

[36] Hu B, Frueh S, Garces HF, Zhang L, Aindow M, Brooks C, et al. Selective hydrogenation of CO2 and CO to useful light olefins over octahedral molecular sieve manganese oxide supported iron catalysts. Applied Catalysis B: Environmental 2013;132–133:54–61. https://doi.org/10.1016/j.apcatb.2012.11.003.

[37] Park S-W, Joo O-S, Jung K-D, Kim H, Han S-H. Development of ZnO/Al2O3 catalyst for reverse-water-gas-shift reaction of CAMERE (carbon dioxide hydrogenation to form methanol via a reverse-water-gas-shift reaction) process. Applied Catalysis A: General 2001;211:81–90. https://doi.org/10.1016/S0926-860X(00)00840-1.

[38] Ateka A, Rodriguez-Vega P, Ereña J, Aguayo AT, Bilbao J. A review on the valorization of CO2. Focusing on the thermodynamics and catalyst design studies of the direct synthesis of dimethyl ether. Fuel Processing Technology 2022;233:107310. https://doi.org/10.1016/j.fuproc.2022.107310.

[39] Ateka A, Pérez-Uriarte P, Gamero M, Ereña J, Aguayo AT, Bilbao J. A comparative thermodynamic study on the CO2 conversion in the synthesis of methanol and of DME. Energy 2017;120:796–804. https://doi.org/10.1016/j.energy.2016.11.129.

[40] Buttler A, Spliethoff H. Current status of water electrolysis for energy storage, grid balancing and sector coupling via power-to-gas and power-to-liquids: A review. Renewable and Sustainable Energy Reviews 2018;82:2440–54. https://doi.org/10.1016/j.rser.2017.09.003.

[41] Khojasteh-Salkuyeh Y, Ashrafi O, Mostafavi E, Navarri P. CO_2 utilization for methanol production; Optimal pathways with minimum GHG reduction cost. Can J Chem Eng 2023;101:5446–59. https://doi.org/10.1002/cjce.24975.

[42] Colbertaldo P, Gómez Aláez SL, Campanari S. Zero-dimensional dynamic modeling of PEM electrolyzers. Energy Procedia 2017;142:1468–73. https://doi.org/10.1016/j.egypro.2017.12.594.

[43] Khojasteh-Salkuyeh Y, Ashrafi O, Mostafavi E, Navarri P. CO2 utilization for methanol production; Part I: Process design and life cycle GHG assessment of different pathways. Journal of CO2 Utilization 2021;50:101608. https://doi.org/10.1016/j.jcou.2021.101608.

[44] Sánchez-Contador M, Ateka A, Aguayo AT, Bilbao J. Direct synthesis of dimethyl ether from CO and CO2 over a core-shell structured CuO-ZnO-ZrO2@SAPO-11 catalyst. Fuel Processing Technology 2018;179:258–68. https://doi.org/10.1016/j.fuproc.2018.07.009.

[45] Ateka A, Portillo A, Sánchez-Contador M, Bilbao J, Aguayo AT. Macro-kinetic model for CuO–ZnO–ZrO2@SAPO-11 core-shell catalyst in the direct synthesis of DME from CO/CO2. Renewable Energy 2021;169:1242–51. https://doi.org/10.1016/j.renene.2021.01.062.

[46] Aguayo AT, Ereña J, Mier D, Arandes JM, Olazar M, Bilbao J. Kinetic Modeling of Dimethyl Ether Synthesis in a Single Step on a CuO−ZnO−Al2O3/γ-Al2O3 Catalyst. Ind Eng Chem Res 2007;46:5522–30. https://doi.org/10.1021/ie070269s.

[47] Molecular Sieve Desiccant | Desiccant Supplier & Manufacturer n.d. https://www.molecularsievedesiccants.com/blogs/how-much-moisture-can-molecular-sieve-adsorb (accessed October 31, 2023).

[48] Deaconu A. Direct DME Synthesis From Natural Gas | EPCM n.d. https://epcmholdings.com/direct-dme-synthesis-from-natural-gas/ (accessed January 7, 2024).

[49] Methanol, 99.9%, for HPLC gradient grade, Thermo Scientific Chemicals, Quantity: 1 L | Fisher Scientific n.d. https://www.fishersci.com/shop/products/methanol-99-9-hplc-gradient-grade-thermo-scientific/AC325740010 (accessed January 7, 2024).

[50] Pim van Keep, Robert Sakko. Flue gas heat recovery through the acid dew point 2019.

[51] Alireza Bahadori, Saeid Mokhatab. Estimating Design Parameters in Propane Refrigerant Systems 2011.

[52] Choi Y, Stenger HG. Water gas shift reaction kinetics and reactor modeling for fuel cell grade hydrogen. Journal of Power Sources 2003;124:432–9. https://doi.org/10.1016/S0378-7753(03)00614-1.

[53] Zheng L, Ambrosetti M, Tronconi E. Joule-Heated Catalytic Reactors toward Decarbonization and Process Intensification: A Review. ACS Eng Au 2023:acsengineeringau.3c00045. https://doi.org/10.1021/acsengineeringau.3c00045.

[54] Bussche KMV, Froment GF. A Steady-State Kinetic Model for Methanol Synthesis and the Water Gas Shift Reaction on a Commercial Cu/ZnO/Al2O3Catalyst. Journal of Catalysis 1996;161:1–10. https://doi.org/10.1006/jcat.1996.0156.

[55] Barati K, Khojasteh-Salkuyeh Y, Ashrafi O, Navarri P. Electrified combined reforming of methane process for more effective CO2 conversion to methanol: Process development and environmental impact assessment. Energy Conversion and Management 2023;287:117096. https://doi.org/10.1016/j.enconman.2023.117096.

[56] Sircar S, Golden TC. Purification of Hydrogen by Pressure Swing Adsorption. Separation Science and Technology 2000;35:667–87. https://doi.org/10.1081/SS-100100183.

[57] Dimian AC, Bildea CS, Kiss AA. Applications in design and simulation of sustainable chemical processes. Amsterda, Netherlands ; Cambridge, MA: Elsevier; 2019.

[58] Mollavali M, Yaripour F, Atashi H, Sahebdelfar S. Intrinsic Kinetics Study of Dimethyl Ether Synthesis from Methanol on γ-Al $_2$ O $_3$ Catalysts. Ind Eng Chem Res 2008;47:3265–73. https://doi.org/10.1021/ie800051h.

[59] Peters MS, Timmerhaus KD, West RE, West RE. Plant design and economics for chemical engineers. 5. ed, international ed. 2004. Boston: McGraw-Hill; 2004.

[60] Hydro-Québec. Hydro-Québec's electricity rates for its electricity distribution activities n.d.

[61] Business Analytiq. Dimethyl Ether price index. Businessanalytiq 2020. https://businessanalytiq.com/procurementanalytics/index/dimethyl-ether-price-index/ (accessed August 6, 2023).

[62] Methanol price index - businessanalytiq n.d. https://businessanalytiq.com/procurementanalytics/index/methanol-price-index/ (accessed September 26, 2023).

[63] H2A: Hydrogen Analysis Production Models n.d. https://www.nrel.gov/hydrogen/h2a-production-models.html (accessed September 26, 2023).

[64] OME Worked Example for the TEA Guidelines for CO2 Utilization. Global CO2 Initiative@UM; 2018. https://doi.org/10.3998/2027.42/147468.

[65] Cost Indices – Towering Skills n.d. https://toweringskills.com/financial-analysis/cost-indices/ (accessed April 6, 2024).

[66] Production Occupations n.d. https://www.bls.gov/oes/current/oes510000.htm (accessed October 2, 2023).

[67] Perry JH, Green DW, Southard MZ, editors. Perry's chemical engineers' handbook. Ninth edition. New York: McGraw-Hill Education; 2019.

[68] Government of Canada CER. CER – Canada's Renewable Power – Canada 2022. https://www.cer-rec.gc.ca/en/data-analysis/energy-commodities/electricity/report/canadas-renewable-power/provinces/renewable-power-canada-canada.html (accessed September 11, 2023).

[69] BC Hydro General Service Business Rates n.d. https://www.bchydro.com/accounts-billing/rates-energy-use/electricity-rates/business-rates.html (accessed September 11, 2023).

[70] NBPower. Énergie NB Power Rates n.d. http://www.nbpower.com/en/products-services/business/rates (accessed September 11, 2023).

[71] dimethyl ether production - RoW - dimethyl ether | ecoQuery n.d. https://ecoquery.ecoinvent.org/3.8/apos/dataset/5593/lci (accessed October 18, 2023).